OXFORD

Cerebral Cortex, 2024, **34**, bhae427
https://doi.org/10.1093/cercor/bhae427
Advance access publication date 27 October 2024
Original Article

Investigating the role of auditory cues in modulating motor timing: insights from EEG and deep learning

Ali Rahimpour Jounghani[1], Kristina C. Backer[2], Amirali Vahid[1], Daniel C. Comstock[3], Jafar Zamani[1], Hadi Hosseini[1], Ramesh Balasubramaniam[2], Heather Bortfeld[2,4,*]

[1]Computational Brain Research and Intervention (C-BRAIN) Laboratory, Department of Psychiatry and Behavioral Sciences, C-Brain Lab, School of Medicine, Stanford University, 1520 Page Mill Rd, Palo Alto, CA 94304, United States
[2]Department of Cognitive and Information Sciences, University of California, Merced, 5200 North Lake Road, Merced, CA 95343, United States
[3]Center for Mind and Brain, University of California, Davis, 267 Cousteau Place, Davis, CA 95618, United States
[4]Psychological Sciences & Cognitive and Information Sciences, University of California, Merced, 5200 North Lake Road, Merced, CA 95343, United States
*Corresponding author: Department of Psychological Sciences & Cognitive and Information Sciences, School of Social Sciences, Humanities and Arts, 5200 N Lake Rd, Merced, CA 95343, United States. Email: hbortfeld@ucmerced.edu

Research on action-based timing has shed light on the temporal dynamics of sensorimotor coordination. This study investigates the neural mechanisms underlying action-based timing, particularly during finger-tapping tasks involving synchronized and syncopated patterns. Twelve healthy participants completed a continuation task, alternating between tapping in time with an auditory metronome (pacing) and continuing without it (continuation). Electroencephalography data were collected to explore how neural activity changes across these coordination modes and phases. We applied deep learning methods to classify single-trial electroencephalography data and predict behavioral timing conditions. Results showed significant classification accuracy for distinguishing between pacing and continuation phases, particularly during the presence of auditory cues, emphasizing the role of auditory input in motor timing. However, when auditory components were removed from the electroencephalography data, the differentiation between phases became inconclusive. Mean accuracy asynchrony, a measure of timing error, emerged as a superior predictor of performance variability compared to inter-response interval. These findings highlight the importance of auditory cues in modulating motor timing behaviors and present the challenges of isolating motor activation in the absence of auditory stimuli. Our study offers new insights into the neural dynamics of motor timing and demonstrates the utility of deep learning in analyzing single-trial electroencephalography data.

Key words: coordination mode; deep learning; ERP; auditory cues; timing indexes.

Introduction

Action-based timing, particularly in rhythmic motor tasks like finger tapping, involves complex neural processes that integrate external sensory cues with internal motor commands. One longstanding challenge in motor neuroscience is the motor equivalence problem, which refers to the phenomenon where motor actions involving different neural and muscular pathways (Lashley 1930) can produce the same behavioral outcome. Motor equivalence highlights the brain's ability to generate flexible motor solutions based on context, sensory input, and individual variability.

In the context of rhythmic behavior, motor equivalence plays a crucial role, as it allows individuals to maintain consistent timing even when the underlying motor patterns differ. For instance, synchronized and syncopated tapping may appear behaviorally similar in terms of motor output (tapping in time with or between an auditory beat), but the neural processes guiding these actions differ significantly due to the varying demands of auditory–motor integration and timing complexity. This distinction is central to understanding the neural mechanisms of motor timing (Kelso et al. 1998).

Our study addresses this issue by investigating how different timing behaviors—synchronization, syncopation, pacing, and continuation—are represented in neural activity and whether these distinct motor patterns can be accurately classified using deep learning techniques. By analyzing the neural signatures of these behaviors at a single-trial level, we aim to shed light on how the brain resolves the motor equivalence problem and adapts its neural output to maintain consistent motor timing. Said differently, even though motor behavior (as evidenced by movement trajectories) is similar for synchronization and syncopation in the presence or absence a stimulus train, the underlying cortical patterns may be quite different.

The human motor system supports motor function and organizes different movement sequences (Rizzolatti and Luppino 2001), enabling actions with a wide range of complexities, including the number of limbs used, number of trajectories involved, sequence length, and relative timing of movement (Wolpert and Ghahramani 2000; Pabst and Balasubramaniam 2018). The ability to accurately and precisely perform time-dependent actions is critical for a variety of skills, such as playing sports or playing a musical instrument. Research has demonstrated that temporal mechanisms in the brain support such behaviors, and there is substantial interest in *how* action-based timing is represented in the central nervous system. In this regard, finger tapping is a reliable and commonly used task for measuring motor performance and evaluating muscle control and motor ability in the upper extremities (Jantzen and Kelso 2007; Witt et al. 2008).

Received: December 15, 2023. **Revised:** October 6, 2024. **Accepted:** October 15, 2024
© The Author(s) 2024. Published by Oxford University Press. All rights reserved. For permissions, please e-mail: journals.permissions@oup.com

Downloaded from https://academic.oup.com/cercor/article/34/10/bhae427/7848901 by UC - Merced user on 30 October 2024

Methodologically, finger tapping allows investigation of the mental timing systems associated with motor actions and feedback mechanisms of varying complexity (Wing and Kristofferson 1973; Sergent 1993; Ivry and Spencer 2004). For example, finger tapping has been used to probe the neural representation and maintenance of timing behavior, where *maintenance* refers to the accurate behavioral maintenance of temporal information following the removal of timing cues. Likewise, finger tapping allows for measurement of relative changes in neural responses that reflect changes in coordination dynamics as participants perform different patterns of tapping with systematically varied levels of difficulty (Spencer et al. 1998; Jantzen et al. 2004).

Here we used a modified finger-tapping task that builds on our previous examination of movement timing (Rahimpour et al. 2020) to investigate the process by which individuals entrain to an external periodic stimulus (i.e. a metronome) and then internally maintain that entrainment (i.e. endogenous rhythmic process). We investigated this across two different timing contexts: synchronized (i.e. on-beat) and syncopated (i.e. off-beat) tapping. Increased activity within neural subsystems associated with timing behavior has been postulated to reflect increases in cognitive demand during coordination of complex action patterns. Examples include internal timing (basal ganglia and cerebellum) (Ivry and Keele 1989; Harrington et al. 1998; Serrien 2008), motor planning and preparation (supplementary motor area [SMA], and dorsal-premotor cortex) (Mayville et al. 2002), and working memory and attention (prefrontal cortex and parietal and occipital areas) (Smith and Jonides 1998; Nobre 2001; Davranche et al. 2011). Other studies indicate that the brain areas recruited during finger tapping include the primary somatosensory-motor cortex (S1/M1), SMA, premotor cortex (PMC), the inferior parietal lobule, basal ganglia, and cerebellum (Nachev et al. 2008; Witt et al. 2008), with different task-specific parameters modulating the particular neural mechanisms that are engaged.

Much progress has been made in identifying neural correlates specific to different forms of sensory-motor synchronization (Repp 2005). For example, the similarities and differences in the neural circuits engaged by tapping to a metronomic tone (i.e. the pacing phase) and continuing to tap without the tone (i.e. the continuation phase) have been investigated using the pacing–continuation paradigm (Serrien 2008). Simple synchronized finger tapping engages the cerebellar-parietal network, while continuation tapping engages prefrontal regions due to its load on working memory (Lewis et al. 2004). More complex sensory-motor synchronization tasks result in greater activation in motor-related areas (pre-SMA, PMC, and cerebellum), as well as stronger coupling to the auditory cortex, such that there is less variability in tap timing when participants have a regular auditory tone—akin to a metronome—to guide the pacing of their action as compared to when they have no such auditory guide (Comstock et al. 2018; Comstock and Balasubramaniam 2018). Indeed, the ability to perceive and respond to temporal periodicities (i.e. timing perception) requires tight coupling of the auditory and motor systems (Grahn and Brett 2007; Chen et al. 2008; Hove et al. 2013; Ebrahimzadeh et al. 2020; Sadjadi et al. 2021) and motor regions, including S1/M1, the SMA, and the anterior cerebellum, are activated during both pacing and continuation tapping (Witt et al. 2008). Meanwhile, frontal networks play an essential role in mediating coordination in tasks with increased complexity (Mayville et al. 2002; Jantzen and Kelso 2007).

To examine the interaction between pattern and timing complexity, Jantzen et al. (2004) used functional magnetic resonance imaging (fMRI) to track cortical hemodynamics as participants performing either synchronized or syncopated finger tapping in response to an auditory cue and then continued their tapping in the absence of that cue. Results revealed that these timing-based behaviors engaged different neural regions depending on the initial pacing context and regardless of its complexity. Our recent findings using functional near-infrared spectroscopy (fNIRS) (Rahimpour et al. 2020) likewise indicate that the cortical activity elicited from timing behavior is task-dependent and that the motor timing network further adapts to the presence or absence of an external stimulus train. In the current study, we explore temporal indicators of the relationship between coordination modes and timing phases and apply deep learning to assess whether the measures of this relationship are robust enough to guide classification.

Neural activation

Tracking neural responsivity to different timing patterns requires a measure that can provide temporal resolution in the millisecond range. Electroencephalography (EEG) is just such a measure; event-related potentials (ERPs) derived from the EEG signal, in particular, measure phase-locked neural activity relative to a stimulus (i.e. auditory tone onset) or response (i.e. finger tap) (Makeig et al. 2004; Lopez-Calderon and Luck 2014). When combined with the continuation paradigm, EEG can be used to track patterns of neural engagement during both the pacing and continuation phases of the continuation task, while the timing of taps provides a behavioral measure of accuracy. For example, Peper et al. (1995) found that stimulus-locked ERPs (i.e. ERPs time-locked to the auditory metronome) during the pacing phase of the continuation paradigm were associated with the motoric act of tapping and were phase-locked to tap onsets. In another study, the amplitude of the event-related changes decreased with increases in tapping cycle frequency (Boonstra et al. 2006). Furthermore, Serrien (2008) found greater EEG coherence—a measure of the degree of similarity in activity across electrodes—at central scalp sites during the continuation relative to the pacing phase of the continuation paradigm, as well as higher variability in tapping accuracy. Because activity in these areas (Clark et al. 2001) is associated with working memory functions, Serrien (2008) interpreted the findings as reflecting increased demand on working memory to maintain the temporal representation of the now-absent auditory stimuli during the continuation phase.

Only a few studies have investigated neural activity associated with both coordination dynamics (synchronization and syncopation) using EEG. Mayville et al. (1999) observed topographical changes in neural activity correlated with an automatic switch of dynamic coordination (from synchronized to syncopated tapping). However, Wallenstein et al. (1995) found that this coordination switch most impacted activity at left central electrode sites and that changes in neural activity increased significantly just prior to this transition. Thus, it seems that the transition from one to the other coordination mode introduces a point of instability in the brain–behavior entrainment pattern due to the change in coordination dynamics.

Finally, an examination of how neural activity coupled with different behavioral movements is contributing to our understanding of action-based timing. For example, Bavassi et al. (2017) observed that the asynchrony between a tone and a tap during synchronized tapping (i.e. the synchronization error) was associated with the latency of specific components revealed by principal component analysis (PCA). In particular, PCA components PC1 and PC2 were analyzed to identify relationships with this asynchrony, although the study did not specify the exact ERP components

Downloaded from https://academic.oup.com/cercor/article/34/10/bhae427/7848901 by UC - Merced user on 30 October 2024

analyzed. This relationship indicated that greater asynchrony corresponded to longer latency, suggesting that increased timing error resulted in delayed neural responses. Smit et al. (2013) likewise found a strong correlation between alpha-band oscillations and the dynamics of tapping behavior, and Nozaradan et al. (2016) reported a link between cortical and behavioral measures of rhythmic movement, finding beat-related steady-state evoked potentials (SSEPs) to be associated with both synchronized and syncopated tapping. SSEPs are neural responses that are phase-locked to rhythmic stimuli and thus reflect how the brain synchronizes with external auditory cues. Researchers also have observed high correlations between the kinematic accuracy of repetitive finger tapping and delta band activity, localized in a central brain area contralateral to the responding hand (Paek et al. 2014), consistent with the negative lateralized readiness potential (LRP) that has likewise been observed in the motor cortex contralateral to the responding hand (Eimer 1998). Overall, there is greater neural responsivity during synchronized than syncopated rhythmic tapping (Chemin et al. 2014), higher amplitude of timing oscillations (reflecting brain activity associated with an increase in rhythmic movement to the metronome) during tapping compared to a listening-only task (Nozaradan et al. 2016), and greater spectral power during synchronizing than listening to rhythmic beat without moving in both auditory and motor areas (Mathias et al. 2020). These findings highlight the relationship between brain responses and action-based timing, showing that neural dynamics, such as oscillations and phase-locked responses, are closely tied to the accuracy and synchronization of rhythmic motor actions like tapping.

Current study

The goal of the present study was to use a temporally sensitive measure of neural activation, EEG, to track neural activity during a tapping task whose complexity varied in both pattern and timing. To this end, we collected EEG data from well-trained participants while they completed a continuation task, similar to the one employed in our prior study (Rahimpour et al. 2020). The task involved both in-phase (i.e. synchronized) and antiphase (i.e. syncopated) tapping. Each form of tapping took place across two phases: first relative to an auditory metronomic tone and then continued without the tone. However, where we blocked trials by tapping pattern in our original study, here, we introduced an alternating design (Pabst and Balasubramaniam 2018) whereby the pattern of tapping alternated trial by trial between synchronization and syncopation, with each trial including both phases: pacing to a tone and continuation without the tone. This change from blocked to alternating trials increased the task difficulty by isolating the specific tapping pattern to a particular trial (Rahimpour Jounghani et al. 2023).

The analytical methods used in the studies reviewed thus far were averaged across trials and did not explore individuals' neurophysiological activity at the single trial level. In particular, the LRP is difficult to extract and is very sensitive to noise, making single-trial analysis difficult. Moreover, intertrial phase coherence can only be calculated from a group of trials (Van Diepen and Mazaheri 2018). Moreover, whereas ERPs can capture the temporal dynamics of neural responses to single events, SSEPs reflect the average response to repeated stimuli over a long period of time; this is a critical point as temporal resolution is one of the main advantages of using EEG for timing studies (De Pretto et al. 2018). In a recent study, Nave et al. (2022) used SSEPs to measure neural responses to musical rhythms that varied in beat salience and showed that beat perception is a subset of rhythm perception, involving the extraction of a regular pulse from a complex auditory signal. However, it is important to note that this method may be more suited to investigating beat perception and may not be as applicable to other forms of timing behavior—a potential limitation.

Although few studies have reported a linear relationship between the amplitude of neurophysiological activity and accuracy of task performance, Nozaradan et al. (2016) found that average asynchrony of taps relative to the guiding tone (i.e. synchronization error) strongly correlates with neural entrainment to a beat. For example, Mathias et al. (2020) observed that the N1 peak latency negatively correlates with the average divergence between the target and realized tap (i.e. mean tap asynchrony), meaning that as mean asynchrony in a complex timing task decreased, stimulus-locked N1 amplitude became more positive (Mathias et al. 2020).

In addition to our discussion of motor equivalence earlier, the interrelation between behavior and the associated neurophysiological dynamics is not linear (Ebrahimzadeh et al. 2019; Vahid et al. 2020), even though most analytic approaches in the literature rely on the assumption of linearity when applying correlational approaches to relate behavioral and neurophysiological data. Moreover, because ERP data are inherently noisy, it is difficult to establish functional connections at the single-participant or single-trial level via statistical techniques alone (Vahid et al. 2020; Ebrahimzadeh et al. 2021). These issues severely limit our capacity to relate specific patterns of neural activity to human behavior. However, these deficiencies may be addressed by employing machine learning techniques.

In particular, we aimed to establish a predictive relationship between neurophysiological activity and behavioral performance at the individual level while participants engaged in distinct action-based timing behaviors. Our primary hypothesis was that neural response as measured by EEG would correspond to the dynamic coordination process that manifests across two forms of timing guidance, exogenous (i.e. during pacing) and endogenous (i.e. during continuation), and during two different tapping behaviors (i.e. synchronization and syncopation). We also aimed to investigate whether and how the individual and single-trial level of neurophysiological activity might predict behavioral accuracy performance across four tapping conditions: synchronized pacing, synchronized continuation, syncopated pacing, and syncopated continuation. Finally, we explore whether the patterns associated with these four tapping conditions can be exploited by deep learning.

Materials and methods

Participants

We recruited 15 healthy volunteers with self-reported normal hearing to participate in the study. All had participated in a prior study in which they performed the same tapping task used here, meaning each had experience with the task. Data from three participants were excluded from the analyses due to a high number of motion artifacts in their EEG data based on visual inspection. Thus, 12 healthy right-handed adult volunteers (mean age 26, range 20 to 41 years) successfully participated in the study. None of the participants reported any neurological or skeletomuscular disorder or injury that would prevent them from performing a timing-based tapping task. The institutional review board approved the protocol for research ethics and the protection of human subjects at the University of California,

Downloaded from https://academic.oup.com/cercor/article/34/10/bhae427/7848901 by UC - Merced user on 30 October 2024

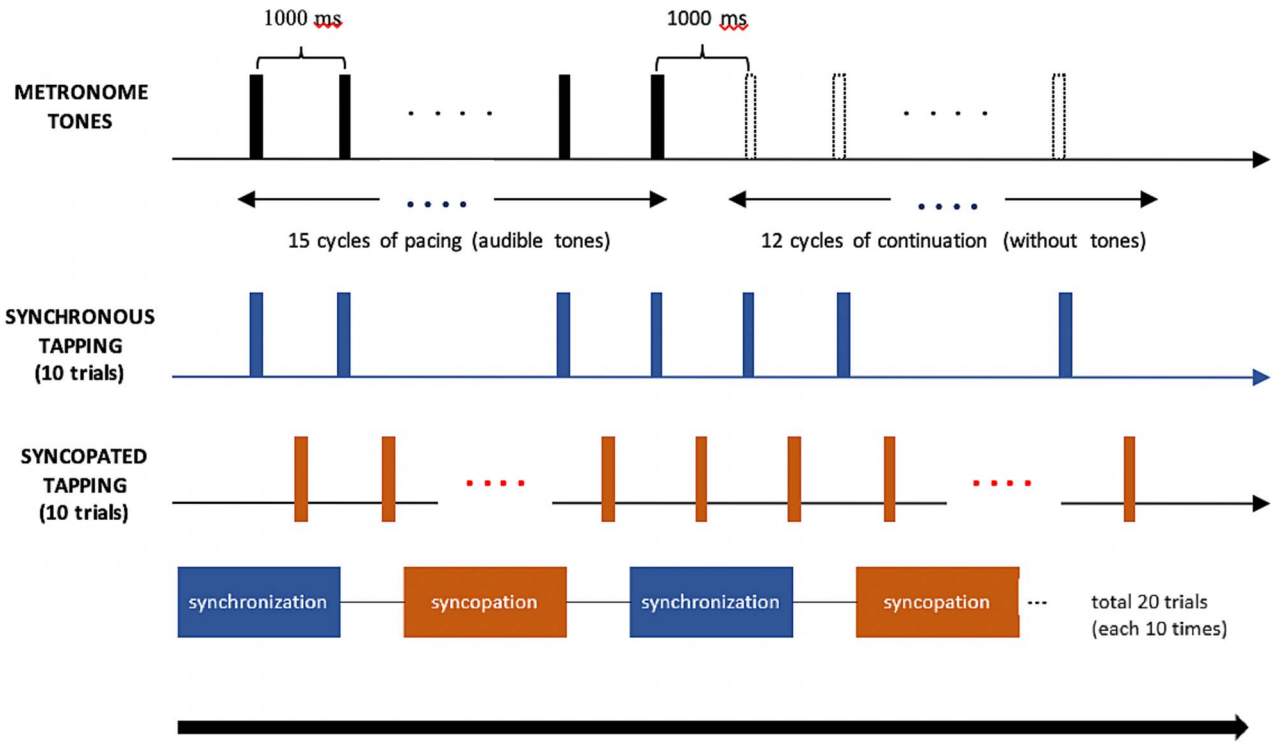

Fig. 1. Schematic of the experimental paradigm adapted from Rahimpour et al. (2020) to perform repetitive right finger tapping in the presence of the auditory metronome in the alternating study design.

Merced. All participants gave informed written consent after the experimental procedures were explained to them.

Stimuli and task

Each participant performed the finger-tapping task using the index finger of their dominant (right) hand in response to a 20-ms long, 1 kHz metronomic tone repeated every 1,000 ms (1 Hz). A 1-s-long tone indicated the end of a trial and the start of a 20-s resting state. A 1-s interonset interval was employed in our study due to its prevalence in previous research investigating rhythm perception and production (e.g. Repp 2005), in addition to our own prior work (Rahimpour et al. 2020; Rahimpour Jounghani et al. 2023). This choice aligns with the optimal internal entrainment range for human synchronization with rhythmic tones, as demonstrated by Drake et al. (2000).

The task involved two patterns of tapping: (i) taps with each tone (synchronization) and (ii) taps between two consecutive tones (syncopation). In order to avoid any neural adaptation to the particular tapping pattern during the performance of the task, we modified the original blocked design introduced by Jantzen et al. (2004) to one in which the tapping pattern alternated between synchronized and syncopated tapping from trial to trial (a syncopation trial always follows a synchronization trial and vice versa) for a total of 10 trials per timing condition (20 trials overall) (see Fig. 1). Regardless of the tapping pattern, within a given trial, tapping was first paced relative to a metronomic tone (15 cycles) and then continued without the tone (12 cycles). Distinct from the designs used in Jantzen et al. (2004) and Rahimpour et al. (2020), participants had experience performing the task in a prior study.

To track tapping behavior, we used a temporally precise device—a smooth metal plate—that did not interfere with the accuracy of participants' tapping during their performance of the task. Two leads were connected to the plate, one connected to a custom-built electronic input device produced from a MakeyMakey kit (Comstock and Balasubramaniam 2018) and the other held by the participant so that with each tap by the participant on the metal plate, the circuit was completed and delivered to the input device, which then sent a signal to the computer via USB, thus registering the tap (Collective and Shaw 2012).

For analytical purposes, we used each finger tap on the plate as the mark of the onset of each behavioral response. The device introduced a temporal delay of approximately 25 ms. The delay is due to the time for the internal circuitry in the MakeyMakey to process the input, which has a built-in delay for input registration to reduce accidental double inputs (similar to a computer keyboard). The 25-ms delay was determined by a method recommended by the MakeyMakey engineers in which a high-speed camera (240 fps) was utilized to simultaneously record the timings of the tap and the corresponding computer registration via a tone output from the computer, a method that computed the delay to be approximately 25 ms (+/−2 ms from the camera frame rate). Thus, we adjusted the time recorded for each response post hoc. Paradigm software was used to present the instructions and to synchronize the onset of each trial with a trigger sent to the EEG data.

EEG data recording

EEG data were continuously recorded with an ANT-Neuro 32 electrode cap with electrodes placed according to the 10–20 International electrode system, assigning Cz as the reference electrode. The data were recorded at a sampling rate of 1024 Hz with electrode impedance below 5 kΩ(Kappenman and Luck 2010). Following acquisition, the EEG data were processed with EEGLAB (Delorme and Makeig 2004) and ERPLAB (Lopez-Calderon and Luck 2014).

Downloaded from https://academic.oup.com/cercor/article/34/10/bhae427/7848901 by UC - Merced user on 30 October 2024

Data processing and analysis

Behavioral measurement

We established two behavioral measures of performance. The first was accuracy asynchrony, defined as the time difference between the target onset and the participant's actual tap (**asynchrony = tap onset − stimulus onset**). In this case, the target time was 0 ms (onset of tone) for synchronization and 500 ms for syncopation. The second was inter-response interval (IRI), defined as the time between two consecutive taps.

We initiated data preprocessing by applying an interquartile range (IQR)–based method to identify and remove outliers in the mean accuracy asynchrony and intertap interval indices. The IQR was calculated as the difference between the 25th percentile (Q1) and the 75th percentile (Q3) of the two behavioral measures. Any data point falling outside 1.5 times the IQR in either direction was flagged as an outlier. After implementing this method, we identified and addressed the outliers to ensure the dataset's integrity. We then handled missing data, with an average of 2.1 instances per timing condition, including single tap outliers and missing taps (1.43 outliers, 2.6 missing taps). To further refine the dataset and maintain balance, we employed a bootstrapping resampling method.

Next, we utilized multiple linear regression (MLR) and piecewise growth curve modeling (using Python's "pwlf" and "StatsModels" libraries) to examine the behavioral effects of timing phase and coordination mode on the dependent variables (mean accuracy asynchronies and IRIs for each participant). This allowed us to model the relationship between timing conditions and motor performance across different phases.

EEG data analysis

Preprocessing

EEG data were preprocessed by first downsampling to 512 Hz and then applying a Butterworth high-pass filter with a cut-off set at 0.1 Hz, an order of 6, and a filter roll-off of 24 dB/octave. Data were then visually examined for artifacts, and corrupted sections were removed. Bad channels were detected and removed using an automated EEGLAB algorithm that compares channels with their surrounding channels (probability measure with z-score threshold set to 4). Four participants had one channel each removed from their data; the other eight participants had no channels removed from their data. Independent component analysis (ICA) was performed using the Runica algorithm (with infomax rotation) within EEGLAB (Bell and Sejnowski 1995) for further artifact rejection. Components were visually inspected, and components related to eye-blink and eye-movement artifacts were removed, resulting in an average of 1.2 components (range: 1 to 2 components) removed per participant. After running ICA, the bad channels (four channels total) were interpolated using spherical interpolation, and the data were re-referenced to the average reference.

We adopted stimulus-locked epochs with the onset of the first tone in each trial as the reference point. Additionally, we accounted for the virtual onset of the continuation phase based on existing literature (Bavassi et al. 2017; Rahimpour Jounghani et al. 2023), which we included in our stimulus-locked analysis. The stimulus-locked epochs served to provide insight into how participants perceived and encoded the presented rhythmic pattern in each trial. Conversely, the response-locked epochs were employed to gain an understanding of how participants planned and executed their tapping response in each trial. Therefore, data were epoched using ERPLAB in two different ways. To create stimulus-locked ERPs, epochs were time-locked to the auditory stimulus onset. Thus, epochs were time-locked to the auditory stimulus onset, and, for response-locked ERPs, epochs were time-locked to the participants' behavioral responses (i.e. taps) after adjusting the triggers 25 ms earlier to account for the delay introduced by the MakeyMakey device, ensuring the taps coincide with their actual occurrence. Both stimulus-locked and response-locked ERPs were epoched from −100 to +500 ms relative to the time-locked event (total number of stimulus-locked epochs = 12,960; response-locked = 10,031). After removing linear trends for an entire epoch, baseline correction was performed to the mean voltage between −100 ms and the stimulus- or response-onset for each epoch.

Further data cleaning was performed at the epoch level with individual epochs removed (mean: 62; range: 9 to 147) if voltage exceeded ±100 μV in any channels for total stimulus-locked and response-locked epochs. Next, we applied a Butterworth low-pass filter with a cut-off at 30 Hz, an order of 4, and a filter roll-off of 24 dB/octave.

Finally, we generated each participant's stimulus-locked and response-locked ERPs for each of the four tapping conditions (i.e. synchronization-pacing, synchronization-continuation, syncopation-pacing, and syncopation-continuation). The total epochs included in the stimulus-locked ERP average per participant were 943±46 (**mean ± SD**) , for synchronized pacing, 912±51 for syncopated pacing, 866 ± 51 for synchronized continuation, and 899 ± 86 for syncopated continuation. Also, the total epochs for response-locked were 741 ± 53, 754 ± 33, 844 ± 76, and 878 ± 29, respectively.

Auditory component removal

In order to test for differences in motor activation across conditions without the interference of the auditory evoked response to the pacing metronome, we used ICA to isolate and remove auditory components before re-running our analyses. ICA was performed using the Runica algorithm (with infomax rotation) on the already cleaned and epoched datasets. For each subject, the primary auditory component was determined by visualizing both the scalp topography of the component and comparing component contributions to the ERP waveforms for stimulus-locked epochs during the pacing conditions and response-locked epochs during the continuation epochs. The component that had the greatest contribution to the auditory evoked response was selected and then checked to ensure that it had a minimal contribution to the response evoked response. Once the primary auditory component was determined, it was removed from the dataset.

Deep learning

Using the conventional average-based ERP method, we did not find a significant main effect of the predictors of the regression model on the averaged ERPs in synchronized pacing ($F_{1,11} = 7.3, P = 0.1, \eta 2 = 0.12$). Additionally, no significant contrast effect was observed between pacing and continuation phases when averaged across coordination modes ($F_{1,24} = 32.36, P = 0.22, \eta 2 = 0.05$). Similarly, no significant contrast effect was found between synchronization and syncopation modes when averaged across timing phases ($F_{1,24} = 19.11, P = 0.41, \eta 2 = 0.01$). To ensure an unbiased approach and avoid cherry-picking specific channels for analysis, we incorporated a deep learning method in our study.

In this study, we examined how well single-trial neurophysiological data at the single-subject level could be used to classify trials into pacing and continuation phases and across two

Downloaded from https://academic.oup.com/cercor/article/34/10/bhae427/7848901 by UC - Merced user on 30 October 2024

coordination modes (i.e. synchronized and syncopated tapping) using EEGNet as a classifier. EEGNet is available for download from https://github.com/vlawhern/arl-eegmodels, and we implemented it using the TensorFlow library in Python to determine whether we could predict behavioral timing conditions based on single-trial EEG data. The methodology and structure of our study were similar to a previous study conducted by Vahid et al. (2020) that examined cognitive control using EEG. To use EEGNet, we converted single-trial EEG data into 2D arrays where channels (C) and time (T) were represented in columns and rows, respectively.

The EEGNet architecture consists of two stages. In the first stage, convolutional filters with a width of 64 samples were applied to generate temporal feature maps, and depth-wise convolution was used to learn D (a parameter that controls the number of spatial filters and covers all EEG channels) for each temporal feature map. Within each temporal map, the model then learned spatial features. After applying temporal and spatial filters, batch normalization followed an exponential linear unit (ELU) activation function. Average pooling over 4-time steps with a stride of 4 was also performed. In the second stage, a separate convolution was used consisting of depth-wise temporal filters with a width of 16, followed by a point-wise convolution. Batch normalization, ELU activation function, average pooling over 8-time steps, and dropout were sequentially applied. Finally, a dense layer with a SoftMax-activation function was used for classification.

We used the "k-fold cross validation" approach (Refaeilzadeh et al. 2009) to evaluate classification performance. We set k to 10 and trained the model for 7466 epochs and then tested it on 747 epochs in the validation set. The number of temporal and spatial filters (F1, D) was set to (4,2), and the batch size was 32. We used the ADAM optimization (Kingma and Ba 2014) to train EEGNet. To account for the unbalanced datasets due to variable numbers of trials across participants and timing conditions, we applied a class weight that was the inverse of the proportion in the training data, with the majority class set to one. We reported the entire confusion matrix and accuracy to evaluate the model's performance.

To identify the EEG timepoints and electrode sites that had the highest impact on the classification decision, we used a "saliency map" approach (Simonyan et al. 2013). The gradient of the classification score was taken before applying the SoftMax-activation function to the input data. This allowed us to generate a map that showed how the model's output changed when there were small changes in the input data at the single-subject level. We averaged saliency maps for each trial belonging to a class and normalized them between 0 and 1 to ensure standardized visualization. Values close to 1 indicated that a particular feature/timepoint strongly contributed to classification accuracy. We calculated a threshold to ensure that the model's classification performance in the 2-class (pacing-continuation) problem was significantly above chance for each participant by assuming that the classification error follows a binomial cumulative distribution (Vahid et al. 2019).

Statistical analyses of behavior–brain relations

For the neural–behavioral analysis, we investigated the relationship between single-trial features extracted via deep learning and participants' behavioral accuracy measures (mean asynchrony and IRI). The relationship was assessed using MLR (via Python's "Scipy" and "StatsModels" libraries) (Seabold and Perktold 2010). We explored linear similarities between the extracted features from stimulus-locked and response-locked ERPs and the behavioral indices to evaluate how well the neural activity aligned with the behavioral performance.

Results

Behavioral results

We first calculated the mean asynchronies and IRIs for the four timing conditions: (i) synchronized pacing, (ii) synchronized continuation, (iii) syncopated pacing, and (iv) syncopated continuation. We then used MLR to estimate a regression model and find the contrast effect between timing conditions post hoc. Moreover, piecewise growth curve approach is calculated to estimate and interpolate the temporal trend of timing conditions on each dependent variable (i.e. mean asynchrony and IRI, separately).

Mean accuracy asynchrony

Our estimated MLR model was calculated to predict mean accuracy asynchrony based on two factors: phase (pacing, continuation) and coordination mode (synchronization, syncopation). A significant main effect of the entire model on the mean synchrony index was found ($F_{1,11} = 11.2, P < 0.02, \eta 2 = 0.49$)in our estimated regression model. There was a main effect of phase on mean accuracy asynchrony ($F_{1,11} = 12.8, P < 0.01, \eta 2 = 0.45$) ,with a 41.12-ms average increase in accuracy asynchrony during continuation compared to pacing. However, the average change in mean accuracy asynchrony for syncopation compared to synchronization was not significant. Thus, the phase variable significantly impacted mean accuracy asynchrony.

For synchronized and syncopated pacing and continuation, the mean accuracy asynchronies were -43.7 ± 13.3 **(ms) (mean ± SD)**, -50.3 ± 116.8 **(ms)**, 12.2 ± 208.3 **(ms)**, and -8.3 ± 206.5 **(ms)**, respectively, as illustrated in Fig. 2A. The results revealed that tapping during the continuation phase was as accurate as but less stable relative to tapping during the pacing phase. We also observed negative mean accuracy asynchrony in the syncopated continuation condition, as well as for both synchronized and syncopated pacing conditions. This describes an averaged accuracy asynchrony that is negative, meaning a participant demonstrates anticipatory timing behavior (rather than reactive tapping). This was only observed in the more complex tapping conditions. In untrained participants, performance in the pacing phase is often less accurate than what we observed in this study. Thus, our results appear to reflect faster rhythmic entrainment in these participants, each of whom had prior experience with the task. Nonetheless, significant differences in mean accuracy asynchrony were observed between pacing and continuation phases for both synchronized ($F_{1,11} = 19.3,\ P < 0.01,\ \eta 2 = 0.39$) and syncopated ($F_{1,11} = 18.1,\ P < 0.01,\ \eta 2 = 0.35$) tapping. Specifically, we found a significant contrast effect between pacing and continuation phases averaged across coordination modes ($F_{1,24} = 6.6, P < 0.04, \eta 2 = 0.25$).

As can be seen in Fig. 2B, the average accuracy asynchrony during the continuation phase was greater than during pacing for both coordination modes. This is consistent with our previous findings (Rahimpour Jounghani et al. 2023) that behavioral performance based on endogenous cues is less accurate than that based on exogenous cues.

We used piecewise growth curve modeling to estimate the fitted model for trial cycles for both pacing and continuation tapping, as shown in Fig. 2C. The top plot in this figure shows the temporal trends for the averaged tapping cycles corresponding to the two coordination modes. The two modes follow each other

Downloaded from https://academic.oup.com/cercor/article/34/10/bhae427/7848901 by UC - Merced user on 30 October 2024

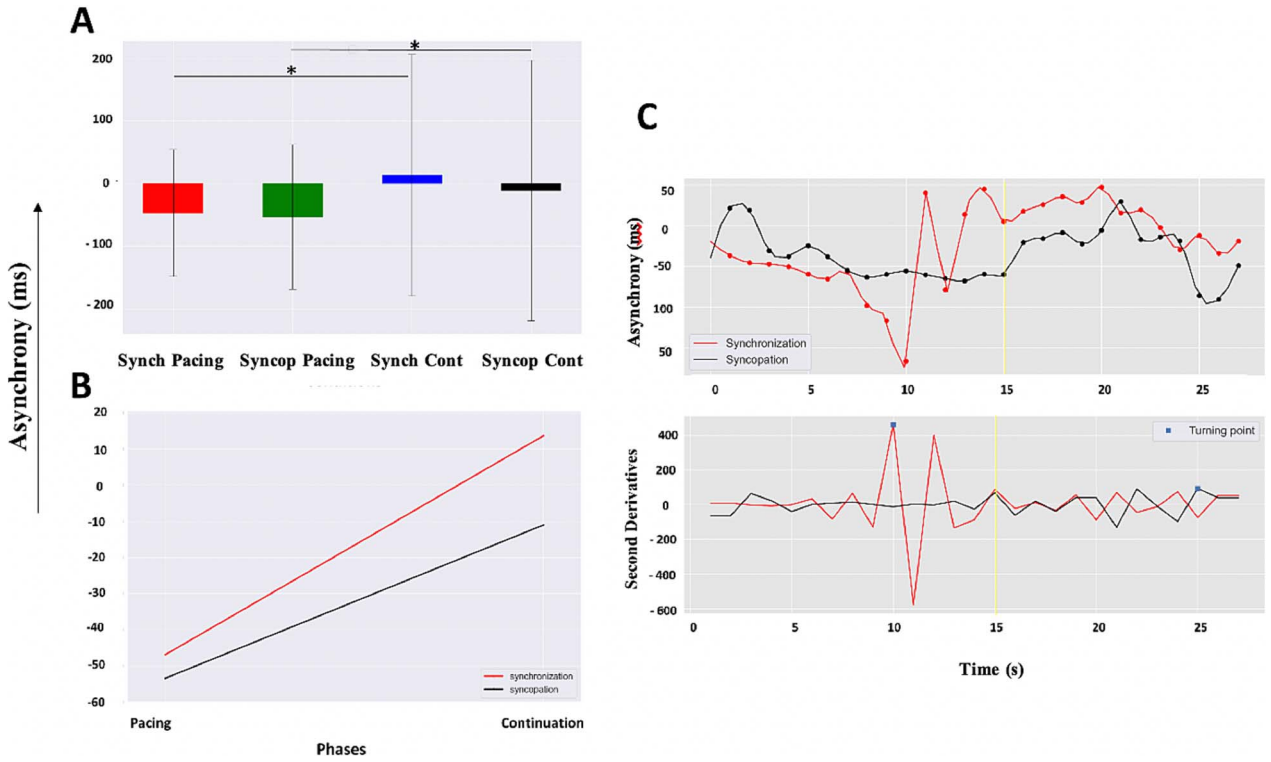

Fig. 2. A) Mean accuracy asynchronies for each timing condition. Error bars show standard deviation (SD). Solid brackets indicate statistically significant comparisons between timing conditions. Synch, Syncop, and Cont indicate synchronized, syncopated, and continuation, respectively. B) Values of mean accuracy asynchrony from each timing condition: Synchronization (top); syncopation (bottom); (C—top) Estimated accuracy asynchrony trend during maintenance (pacing followed by continuation). (C—bottom) Second derivatives of the corresponding trends locating the turning points (square marks) in: synchronization; syncopation; vertical solid line represents continuation phase onset.

closely across the first 10 s, at which point the trend toward synchronization across time reveals more variation than syncopation (during timepoints 10 to 17 s); subsequent to that, the time series for synchronization stabilizes (during timepoints 17 to 27 s), albeit to a pattern closer to that seen during syncopation. This means that although the behavioral accuracy of syncopation is less accurate overall, it is stably so. The bottom plot shows the second derivative of the trends specifying the turning point estimated by our interpolated model. As can be seen, the estimated turning point for both synchronized and syncopated tapping occurs at 10 s (5 s before the phase change timepoint) and at 25 s (10 s after phase transition). This effect is consistent with our previous finding reported in Rahimpour Jounghani et al. (2023).

Behavioral IRI

We estimated the MLR model's ability to predict IRI based on coordination mode and phase. A significant effect of each of the independent variables on the mean accuracy asynchrony index was found ($F_{1,11} = 5.8, P < 0.05, \eta 2 = 0.31$) in our estimated regression model. Moreover, there was a marginally significant main effect of phase on IRI ($F_{1,11} = 5.13, P = 0.05, \eta 2 = 0.27$).

As shown in Fig. 3A, the average performance of trained participants was very consistent for all timing conditions, where IRI represents how evenly spaced taps are consistent. However, the stability of performance decreases as the timing complexity increases. For synchronized and syncopated pacing and continuation, the IRIs were 997.1 ± 43.2 (ms) (mean ± SD), 998.4 ± 45.8 (ms), 1000.8±62.9 (ms), and 1016.3±71.1 (ms), respectively. The only significant difference we observed was between the syncopated pacing and the syncopated continuation ($F_{1,11} = 6.43, P < 0.05, \eta 2 = 0.23$) conditions. As can be seen in Fig. 3B, the IRI index in the syncopated continuation condition was higher than in other conditions (consistent with Rahimpour et al.'s 2020 finding). Finally, we found an interaction between phase and coordination mode ($F_{3,11} = 6.51, P = 0.04, \eta 2 = 0.18$), which is also consistent with our previous findings (Rahimpour et al. 2020).

We used piecewise growth curve modeling to estimate the fitted model of averaged pacing and continuation tapping trial cycles, as shown in Figs. 3C. The top plot in this figure shows the temporal trends for the averaged tapping cycles corresponding to the two coordination modes. The trend for synchronization over time was consistent and close to an ideal IRI value (i.e. 1,000 ms); however, abrupt changes were observed in the 10- to 17-s time range, particularly before the continuation onset timepoint. Similar to mean accuracy asynchrony, the temporal trends for the two coordination modes follow each other very closely at the beginning and at the end of the cycles. The bottom plot shows the second derivative of the trends, which specifies the turning point estimated by our interpolated model. As can be seen, the estimated turning point for synchronized and syncopated tapping occurred at 11 s (4 s before the phase transition timepoint) and at 12 s (3 s after phase transition). These observations are consistent with the findings (from the fNIRS alternating study) reported in Rahimpour Jounghani et al. (2023).

The identification of a turning point is crucial, as it enables us to determine whether the data-driven transition from pacing to continuation aligns with the intended experimental manipulation (i.e. the switch from pacing to continuation). These results underscore the importance of predicting action-based timing behavior at the single-trial level using neurophysiological data, as this

Downloaded from https://academic.oup.com/cercor/article/34/10/bhae427/7848901 by UC - Merced user on 30 October 2024

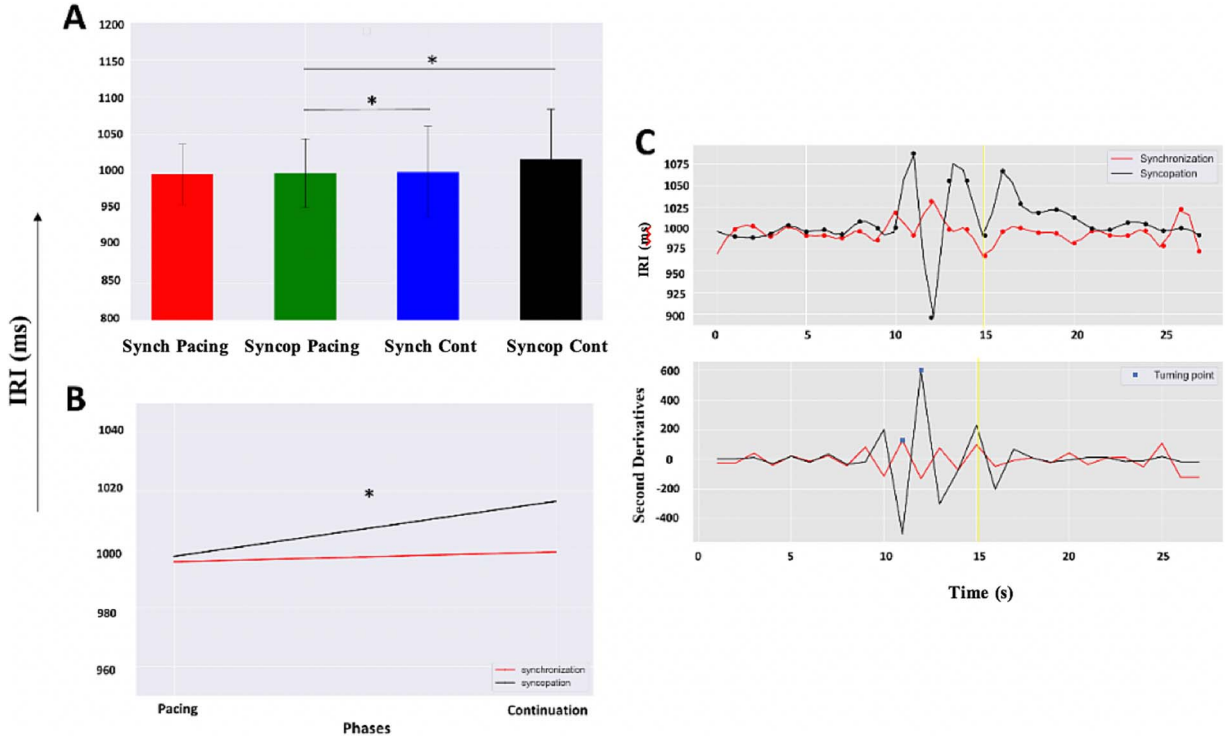

Fig. 3. A) IRIs of each timing condition (i.e. from left to right: synchronized pacing, syncopated pacing, synchronized continuation, and syncopated continuation). Error bars show SD. Solid brackets indicate statistically significant comparisons between timing conditions. B) Averaged IRI values from each timing condition: syncopation (top); synchronization (bottom); (C—top) Estimated IRI trend during maintenance (pacing followed by continuation). (C—bottom) Second derivatives of the corresponding trends locating the turning points (square marks) in: synchronization; syncopation; vertical solid line represents continuation phase onset.

approach helps to account for potential misalignments between the designed experimental phases and the patterns that emerge from the data-driven analysis.

Neural results

In this study, we first aimed to use deep learning to extract neurophysiological features that predicted brain states. Because the significant contrasts of behavioral accuracy (i.e. mean accuracy asynchrony and IRI) were only observed for two timing phases and not for the two coordination modes, we aimed to classify pacing and continuation phases for each coordination mode (synchronization and syncopation). Finally, we measured the monotonic association between the extracted neurophysiological and behavioral indexes (i.e. mean asynchrony and IRI) using Spearman's rank correlation method.

Feature extraction and classification

As described in the Materials and Methods section, we used deep learning to investigate whether classification emerged within electrodes for stimulus- and response-locked ERPs. Deep learning predicts the presence of neurobiological markers to classify behavioral phases. Since the behavioral data revealed the performance differences modulated with pacing–continuation behavioral phases, this factor was considered in the deep learning step. Therefore, the study focused on the 2-class problem of pacing-continuation within two coordination dynamics—synchronization and syncopation—to train the deep learning architecture (EEGNet) on a training dataset. The trained model was then applied to the test/validation dataset to determine how well it identified the two different timing conditions for each coordination mode. That is, for evaluating classification performance, we used the "10-fold cross validation" approach (see Materials and Methods for more details). The chance level of our 2-class problem would be 50% classification accuracy. We thus calculated a threshold that indicated classification accuracies significantly above chance by assuming the classification error conformed to a binomial cumulative distribution.

Pacing-continuation classification

Synchronization coordination mode

The average accuracy of trial class prediction given stimulus-locked, single-trial EEG data was 70% (SD = 28%), which was 20% (SD = 17.2%) higher than the individual chance level [$t(11) = 16.3; P = 0.02, \eta 2 = 0.44$]. The confusion matrix for the 2-class problem is shown in Fig. 4A. Rows show real ("true") labels, while the columns show the classification labels, which were generated by the model based on the single-trial EEG data. The average prediction accuracy of 70% can be seen in the confusion matrix (see diagonal from top left to bottom right of the confusion matrix). Thus, performance was above chance and then correct predictions outnumbered incorrect predictions. In particular, synchronized continuation trials were incorrectly classified as synchronized pacing for only 26% of the cases. In contrast, synchronized continuation trials were correctly classified as such in 74% of cases. Generally, the confusion matrix shows that the deep learning approach employed here can classify trial class (experimental timing phase) based on single-trial data.

Figure 4B presents separate visualization ("saliency") maps for each of the two classes of pacing and continuation. As can be seen in Fig. 4B, the FC1 electrode strongly contributed to classification accuracy in the time window from 110 to 180 ms. Moreover, we observed contribution to classification for C4 and T8 in the time

Downloaded from https://academic.oup.com/cercor/article/34/10/bhae427/7848901 by UC - Merced user on 30 October 2024

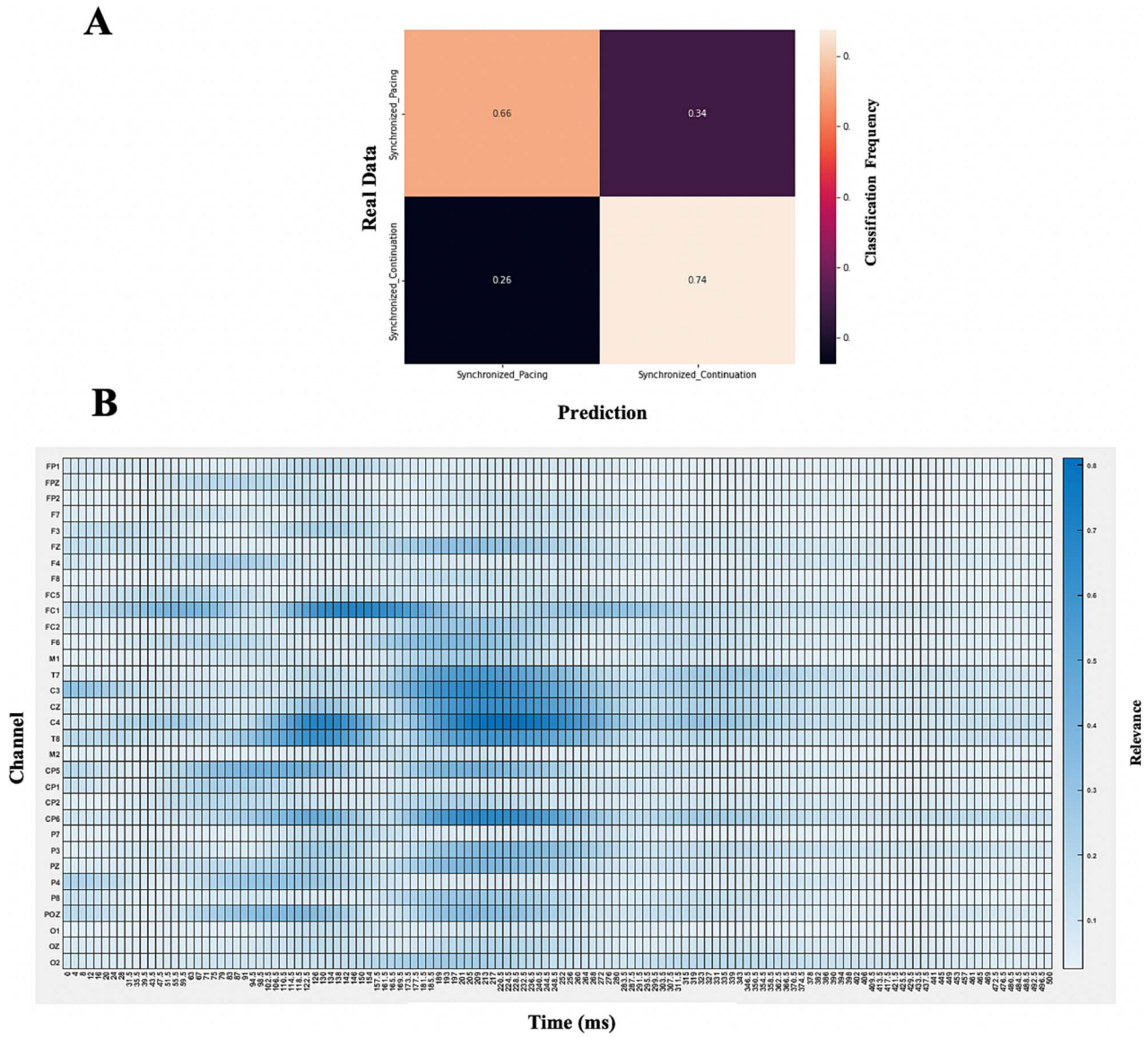

Fig. 4. A) Confusion matrix showing the classification results for the stimulus-locked trials of the pacing (the same as continuation) in synchronization mode. Color shadings and number in the matrix denote the frequency at which the read data "true" label was classified into one of the two possible predicted classes. B) Visualization maps showing the relevance of all timepoints and electrodes for the classification of two classes of pacing and continuation stimulus-locked trials in synchronization mode. Values close to 1 indicate that the specific feature at the specific timepoints contributes most to classification accuracy. The *x* axis denotes the time in ms after auditory stimulus presentation. The *y* axis indicates the different electrode sites.

range from 110 to 140 and 190 to 260 ms, as well as for T7, C3, and Cz in the time range from 190 to 260 ms. Importantly, this was the case for both classes of pacing and continuation trials. The ERP plots showing activity at these electrodes can be seen in Fig. 5. The identified time window overlaps with the auditory N1 and P2 peak latency component, which reflects auditory stimulus processing. Therefore, it appears that auditory attention contributes to the predictive power of stimulus-locked single trials from the synchronized form of the experiment. However, we did not observe meaningful classification of response-locked single trials of synchronization mode. Furthermore, the initial positivity in channels T7 and T8 is likely a polarity reversal of the N1b and P2 components seen on top of the head, rather than a reflection of the N1c/Ta/Tb subcomponents, which are typically focal in temporal electrodes and exhibit sensitivity to alterations in pitch and timbre (Näätänen and Picton 1987). Our primary emphasis is directed toward the N1b component, which is the predominant and enduring facet of the N1 complex, elucidating stimulus onset processing. The auditory N1b component (during synchronized pacing, see Fig. 5 top-left topography) is likely co-occurring with a motor-timing process that results in a widespread negativity across the scalp. However, we acknowledge that the N1c/Ta/Tb subcomponents may exert their influence on rhythm perception and production (Näätänen and Picton 1987).

Syncopation coordination mode

Stimulus-locked ERPs

The average accuracy of trial-level classification on the basis of the stimulus-locked single-trial EEG data was 70% (SD = 26%) and thus 20% (SD = 19.2%) higher than the individual chance level [$t\ (11) = 15.3; P = 0.02, \eta 2 = 0.51$]. The confusion matrix for the 2-class (pacing–continuation) problem is shown in Fig. 6A. Rows show real ("true") labels and columns show classification labels as predicted on the basis of the single-trial EEG data.

Downloaded from https://academic.oup.com/cercor/article/34/10/bhae427/7848901 by UC - Merced user on 30 October 2024

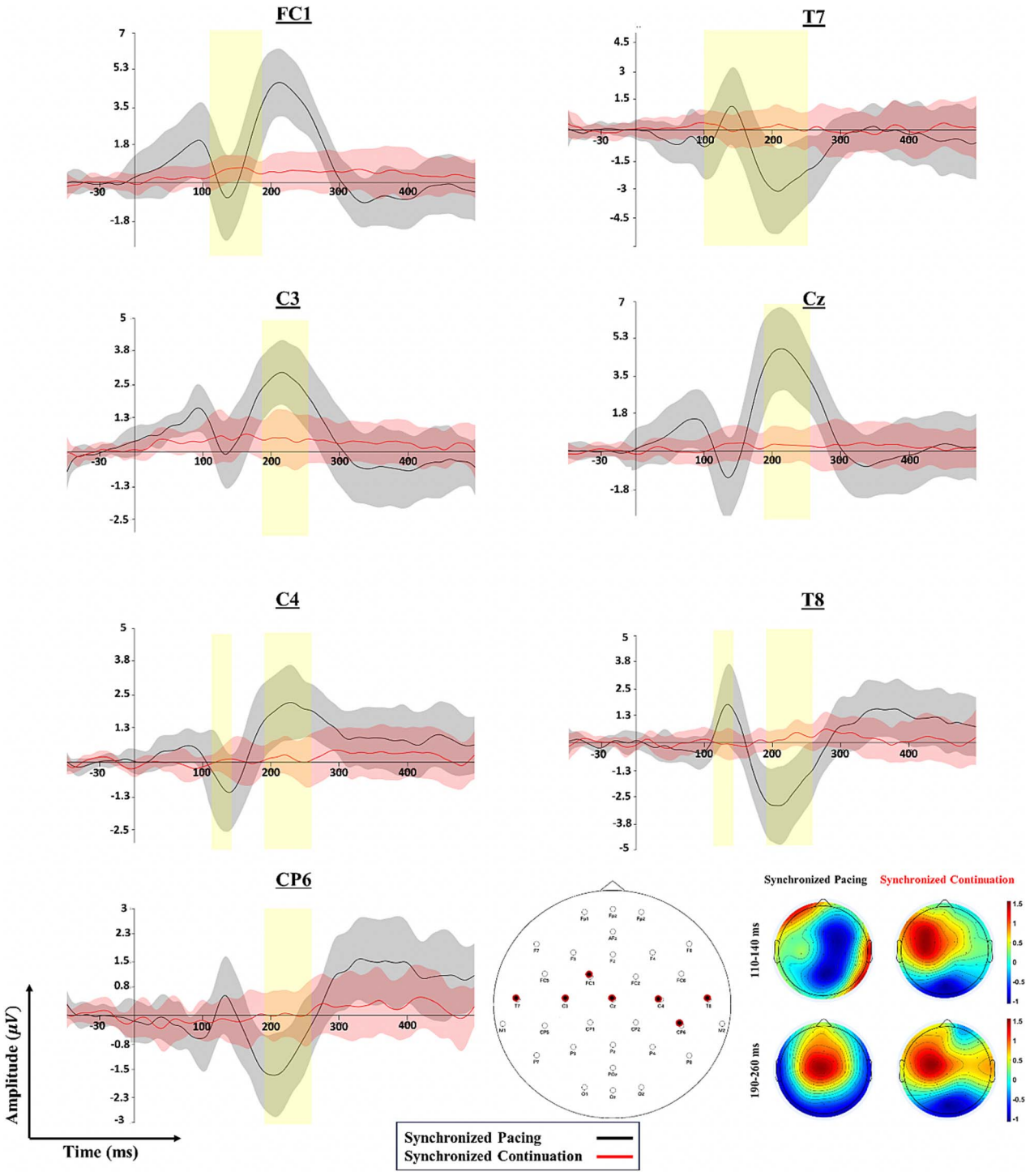

Fig. 5. Stimulus-locked ERPs at the electrode sites contributing most to classification accuracy (for pacing vs. continuation) during synchronized tapping in the deep learning model. The *x* axis indicates the time in ms after auditory stimulus-locked presentation. The curves indicate the averaged ERP values for pacing and continuation phases, respectively. The shading indicates the SE across the time. The *y* axis indicates the voltage in μV (note that the scaling of the *y* axis differs between the plots). The shading shows the time interval that was found to contribute strongly to classification performance in the deep learning network. The scalp maps in bottom right side indicate the amplitude of electrode sites in extracted N1 peak latency (time range: 110 to 140 ms) and P2 peak latency (190 to 260 ms). Please note that the *y* axis limits are scaled to the data amplitudes for each plot.

As can be seen in the confusion matrix, the average prediction accuracy was 70% (see diagonal from top left to bottom right in the confusion matrix). This was above chance and substantially larger than the percentage of incorrect predictions. For example, syncopated continuation trials were only incorrectly classified as syncopated pacing in 25% of cases, meaning syncopated continuation trials were correctly classified as such in 75% of cases.

Figure 6B presents separate visualization ("saliency") maps for each of these two classes of pacing and continuation. As can be seen in Fig. 6B, C3, C4, T8, and CP6 electrodes strongly contributed to classification accuracy of timing phase in the time

Downloaded from https://academic.oup.com/cercor/article/34/10/bhae427/7848901 by UC - Merced user on 30 October 2024

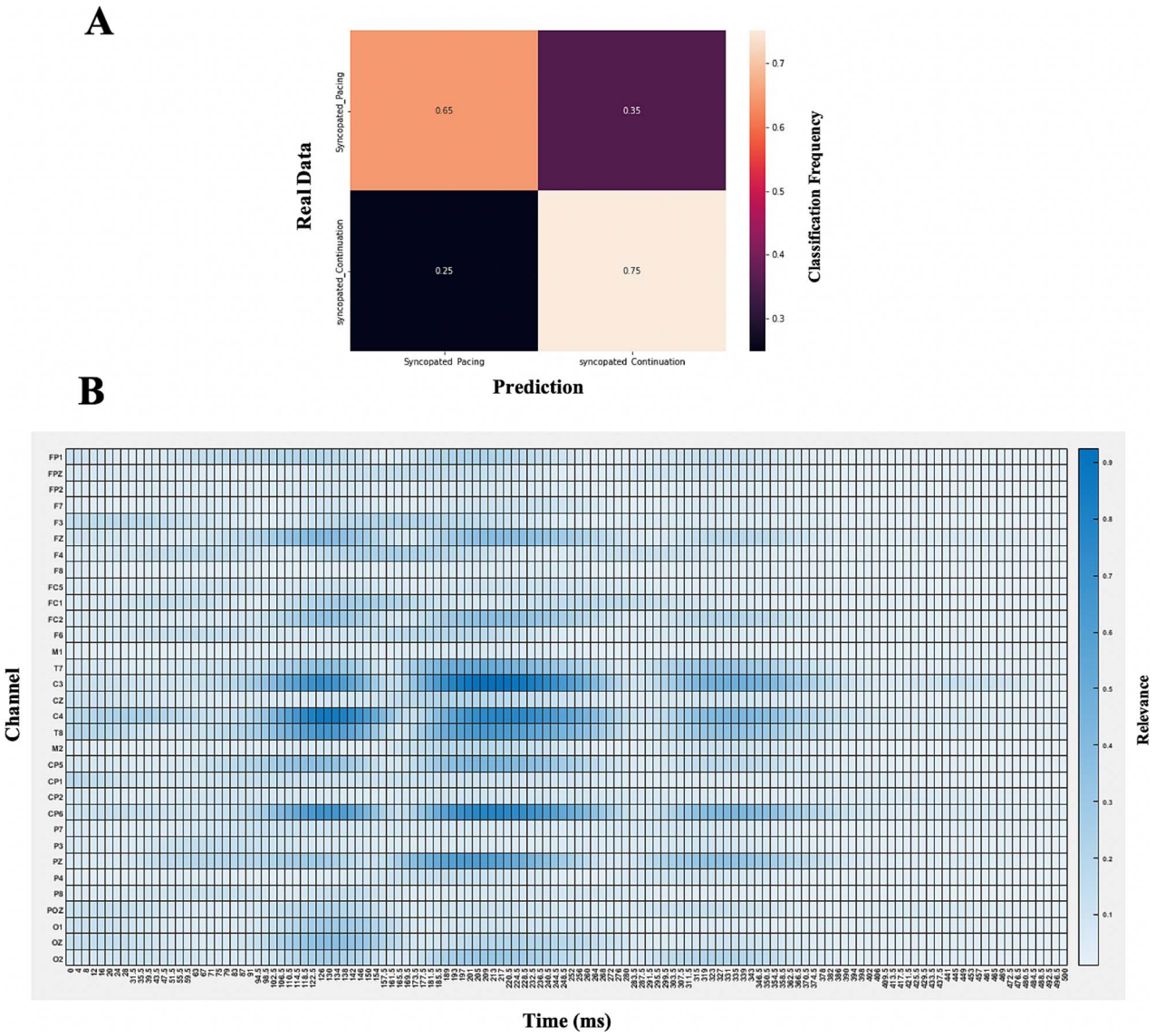

Fig. 6. A) Confusion matrix showing the classification results for the pacing in the syncopation coordination mode. Color shadings and number in the matrix denote the frequency at which the read data "true" label was classified into one of the two possible predicted classes. B) Visualization maps showing the relevance of all timepoints and electrodes for classification between two classes of pacing trials and continuation stimulus-locked trials in syncopation mode. Values close to 1 indicate that the specific feature at the specific timepoints contributes most to classification accuracy. The x axis denotes the time in ms after auditory stimulus presentation. The y axis indicates the different electrode sites.

window from 115 to 135 and 190 to 250 ms. Electrode Pz also contributed to the classification accuracy in the time window 190 to 250 ms. Crucially, this was the case for both classes of pacing and continuation trials. The ERP plots showing activity at these electrodes are given in Fig. 7. The identified time window overlaps with the auditory N1 and P2 ERP peak latency components, which reflects auditory processes. Therefore, auditory attention appears to be predictive of which phase of tapping a person is in given syncopated coordination mode.

Response-locked ERPs

The average accuracy of trial-level classification prediction on the basis of the response-locked single-trial EEG data was 66% (SD = 29.5%) and thus 16% (SD = 23.2%) higher than the individual chance level [t (11) = 18.7; $P = 0.046$, $\eta 2 = 0.24$]. The confusion matrix for the 2-class (pacing–continuation) problem is shown in Fig. 8A. Rows show real ("true") label; the columns show the classification label, which was predicted on the basis of the single-trial EEG data. As can be seen in the confusion matrix, the average prediction accuracy was 66% (see diagonal from top left to bottom right in the confusion matrix). Syncopated pacing trials were only incorrectly classified as syncopated continuation in 28% of cases. In contrast, syncopated pacing trials were correctly classified as such in 72% of cases. Generally, the confusion matrix shows that the deep learning approach employed here was able to classify trial class (i.e. phases) on the basis of single-trial data.

Figure 8B presents separate visualization ("saliency") maps for each of these two classes of pacing and continuation. As can be seen in Fig. 8B, the strong contribution for classification accuracy can be observed in the following electrodes and time ranges: Fz: 80 to 130 ms; FC1: 60 to 100 ms; C3: 110 to 140 ms, 200 to 270 ms; C4: 90 to 140 ms, 200 to 250 ms; T8:100 to 130 ms, 210 to 250 ms; CP5: 0 to 20 ms, 80 to 120 ms, 200 to 220 ms; CP6: 115 to 145 ms; 220 to 280 ms; and Pz: 50 to 100 ms, 180 to 220 ms. Crucially, this was the case for both classes of pacing and continuation trials. The

Downloaded from https://academic.oup.com/cercor/article/34/10/bhae427/7848901 by UC - Merced user on 30 October 2024

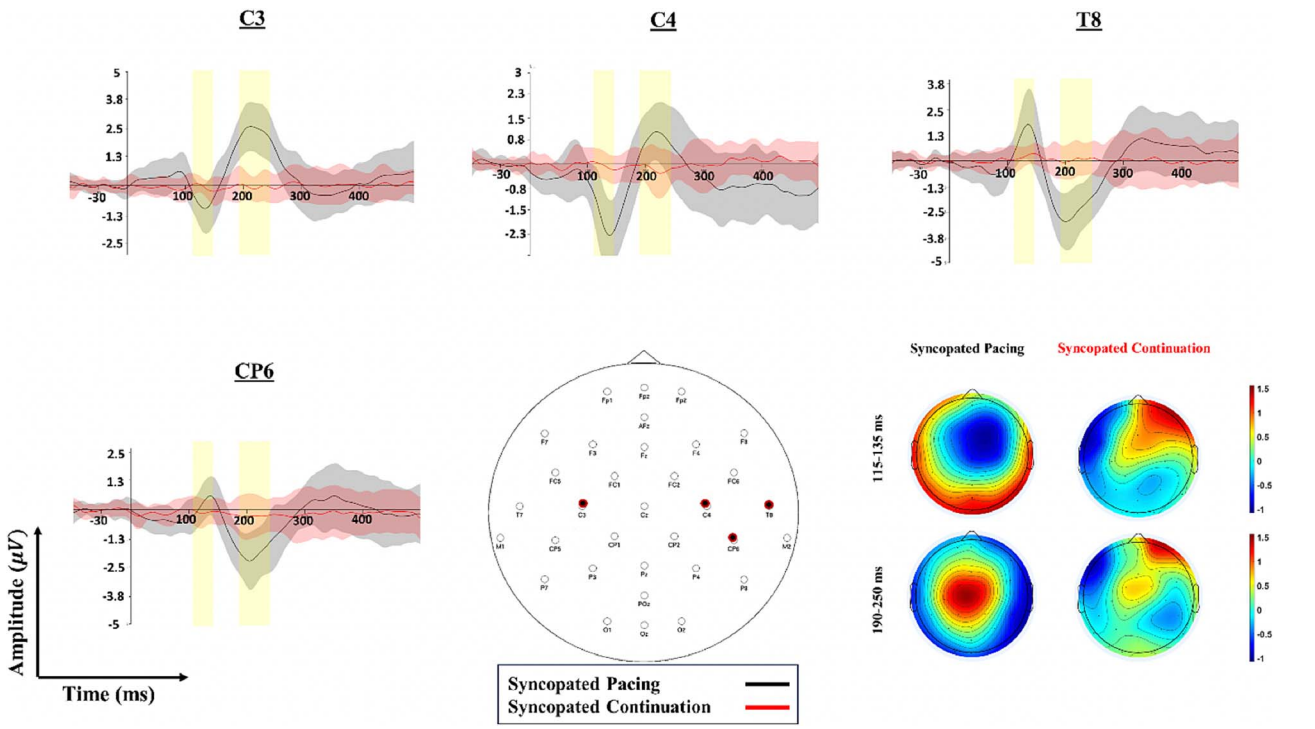

Fig. 7. Stimulus-locked ERPs at the electrode sites contributing most to classification (pacing–continuation phases) accuracy of syncopation mode in the deep learning model. The *x* axis indicates the time in ms after auditory stimulus-locked presentation. The curves indicate the averaged ERP values of pacing and continuation phases, respectively. The shading indicates the SE across the time. The *y* axis indicates the voltage in μV (note that the scaling of the *y* axis differs between the plots). The shading shows the time interval that was found to contribute strongly to classification performance in the deep learning network. The scalp maps in the bottom-right side indicate the amplitude of electrode sites in extracted N1 (time range: 115 to 135 ms) and P2 peak latency component (190 to 260 ms). Please note that the *y* axis limits are scaled to the data amplitudes for each plot.

ERP plots showing activity at these electrodes are given in Fig. 9. The identified time window overlaps with specified time range of motor components, which is known to reflect motor processes. Therefore, motor response processes are predictive of response-locked timing phases in syncopation mode.

It should be noted that the classification accuracy between synchronized and syncopated pacing was not above the chance level (for stimulus-locked single-trial ERPs: 55%; response-locked: 60%) and between synchronized continuation and syncopated continuation was not acceptable (for stimulus-locked single-trial ERPs: 52%; response-locked: 61%).

Classification of timing conditions after removing auditory components

We also fed the auditory component-removed ERPs to deep learning to test for differences in motor activation between two coordination modes in the pacing phase as well as between phases (pacing vs. continuation) in both synchronization and syncopation modes separately. The classification accuracy between synchronization and syncopation modes was low, with correct predictions not outnumbering incorrect predictions (for stimulus-locked single-trial ERPs: 45%; response-locked: 53%). Similarly, the classification accuracy between phases in the continuation paradigm was low (for stimulus-locked single-trial ERPs: 49%; response-locked: 48%). These results suggest that the auditory component may be driving the differentiation effect we observed in the original ERP data between pacing and continuation phases. Without the auditory contribution, neural responses did not reliably differentiate these phases, highlighting the importance of auditory cues in modulating motor activation during timing task.

Relations between single-trial ERPs and behavioral measures

Based on the findings of single-trial ERP classification, we predicted that individual differences in extracted cortical features (contributed auditory and motor components) would correlate with behavioral indices. Thus, separate MLR analyses were conducted to examine the relationship between individual differences in extracted single-trial features and our behavioral accuracy measures (i.e. mean accuracy asynchrony and IRI). The behavioral mean accuracy asynchrony and IRI were the dependent variables in the regression model ($n = 12$). The independent variables in the model are the extracted single-trial amplitudes in each electrode sites that contributed to the classification. We explored all possible correlations and plotted the ones in which the relationship was statistically significant.

Mean accuracy asynchrony

The MLR analysis yielded a model with $\mathbf{r_s} = -0.42, F\ (1, 11) = 6.33, P = 0.03$ with the average stimulus-locked ERP emerging as the only significant unique predictor of mean accuracy asynchrony performance in synchronized pacing. A scatterplot showing the negative correlation between the extracted stimulus-locked ERP amplitude (included P2 peak latency: 180 to 220 ms) and mean accuracy asynchrony is shown in Fig. 10. In support of our general hypothesis about the predictive power of single-trial ERPs, stronger neural activity in CP6 electrode site relates to more negative mean accuracy asynchrony in the synchronized pacing condition.

We also found a correlation between the average response-locked ERP emerging as the predictor of mean accuracy

Downloaded from https://academic.oup.com/cercor/article/34/10/bhae427/7848901 by UC - Merced user on 30 October 2024

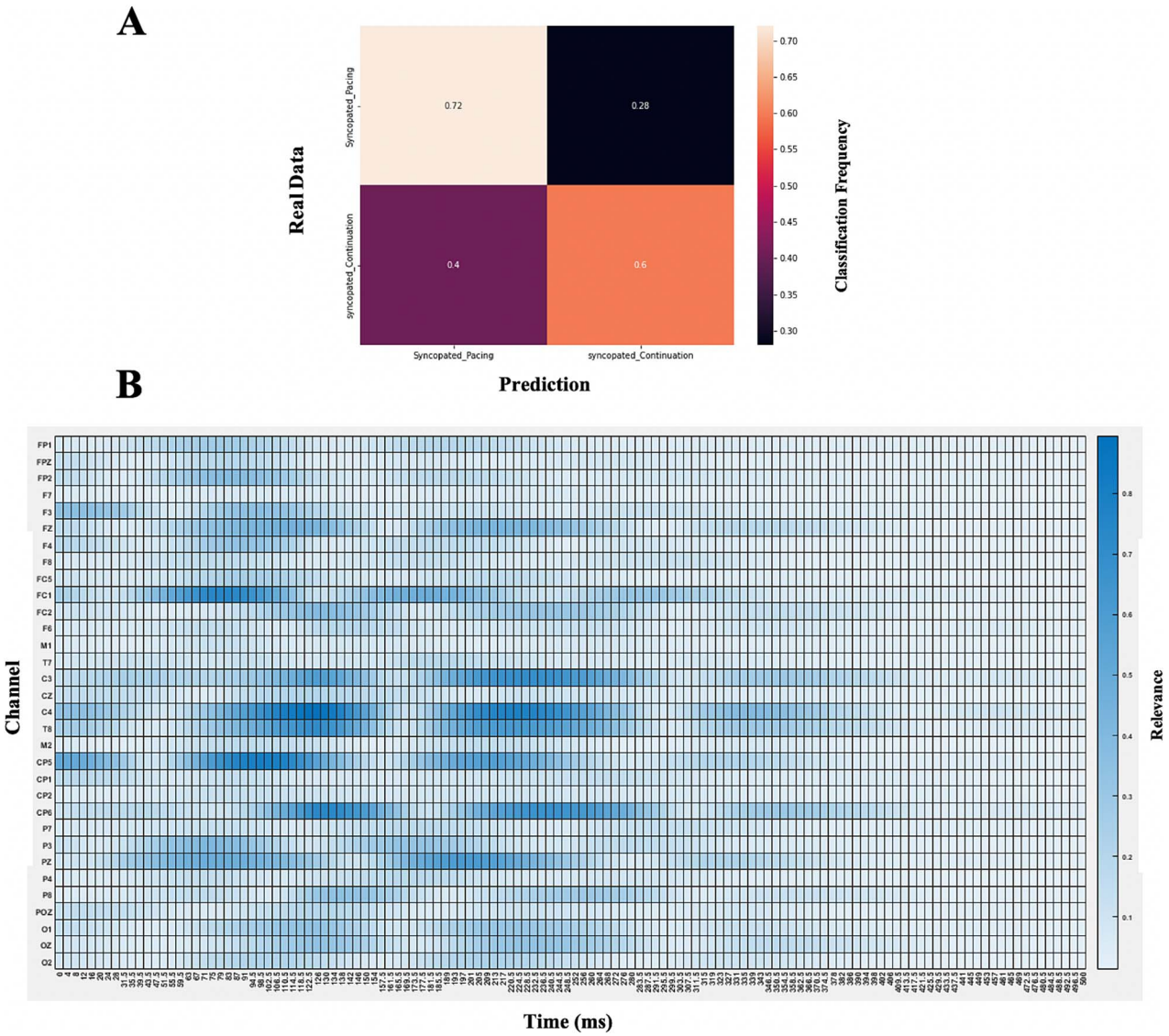

Fig. 8. A) Confusion matrix showing the classification results for the response-locked trials of the pacing and continuation in syncopation mode. Color shadings and number in the matrix denote the frequency at which the read data "true" label was classified into one of the two possible predicted classes. B) Visualization maps showing the relevance of all timepoints and electrodes for classification between two classes of pacing trials and continuation tapping response-locked trials in syncopation mode. Values close to 1 indicate that the specific feature at the specific timepoints contributes most to classification accuracy. The x axis denotes the time in ms after tapping response presentation. The y axis indicates the different electrode sites.

asynchrony $[r_s = 0.39, F\ (1, 11) = 7.24, P = 0.04]$ in syncopated pacing. A scatterplot showing the positive correlation between the extracted tapping-locked ERP amplitude in FC1 electrode site extracted from the deep learning method and mean accuracy asynchrony is shown in Fig. 11. The greater neural activity at the FC1 electrode site relates to lower mean accuracy asynchrony in the syncopated pacing condition.

In addition, a correlation was observed between averaged extracted single-trial response-locked ERP emerging as the predictor of mean asynchrony $[r_s = -0.56, F\ (1, 11) = 6.77, P = 0.01]$ in syncopated continuation condition. A scatterplot showing the negative correlation between the extracted tapping-locked ERP amplitude at the Pz electrode site extracted from our deep learning model and mean accuracy asynchrony is shown in Fig. 12. Thus, stronger neural activity at the Pz electrode site related to higher mean accuracy asynchrony in the syncopated continuation condition.

IRI

We estimated our regression model in syncopation mode and found strong correlation $r_s = 0.66, F\ (1, 11) = 9.05, P = 0.01$ with the average auditory-locked ERP in Pz as another predictor of IRI performance. A scatterplot showing the strong positive correlation between the extracted stimulus-locked ERP amplitude (included P2 peak latency: 180 to 220 ms) and IRI index is shown in Fig. 13, indicating that stronger neural activity at the Pz electrode site relates to higher IRI in the syncopated pacing condition.

Moreover, this analysis yielded a model with $r_s = -0.55$, $F\ (1, 11) = 7.69, P = 0.01$ with the average selective response-locked ERP emerging as the significant predictor of IRI performance accuracy. A scatterplot indicating the negative correlation between the extracted ERP amplitude at the T8 electrode site and IRI accuracy is shown in Fig. 14. Thus, stronger neural activity at the T8 electrode site relates to lower IRI in the syncopated pacing condition.

Downloaded from https://academic.oup.com/cercor/article/34/10/bhae427/7848901 by UC - Merced user on 30 October 2024

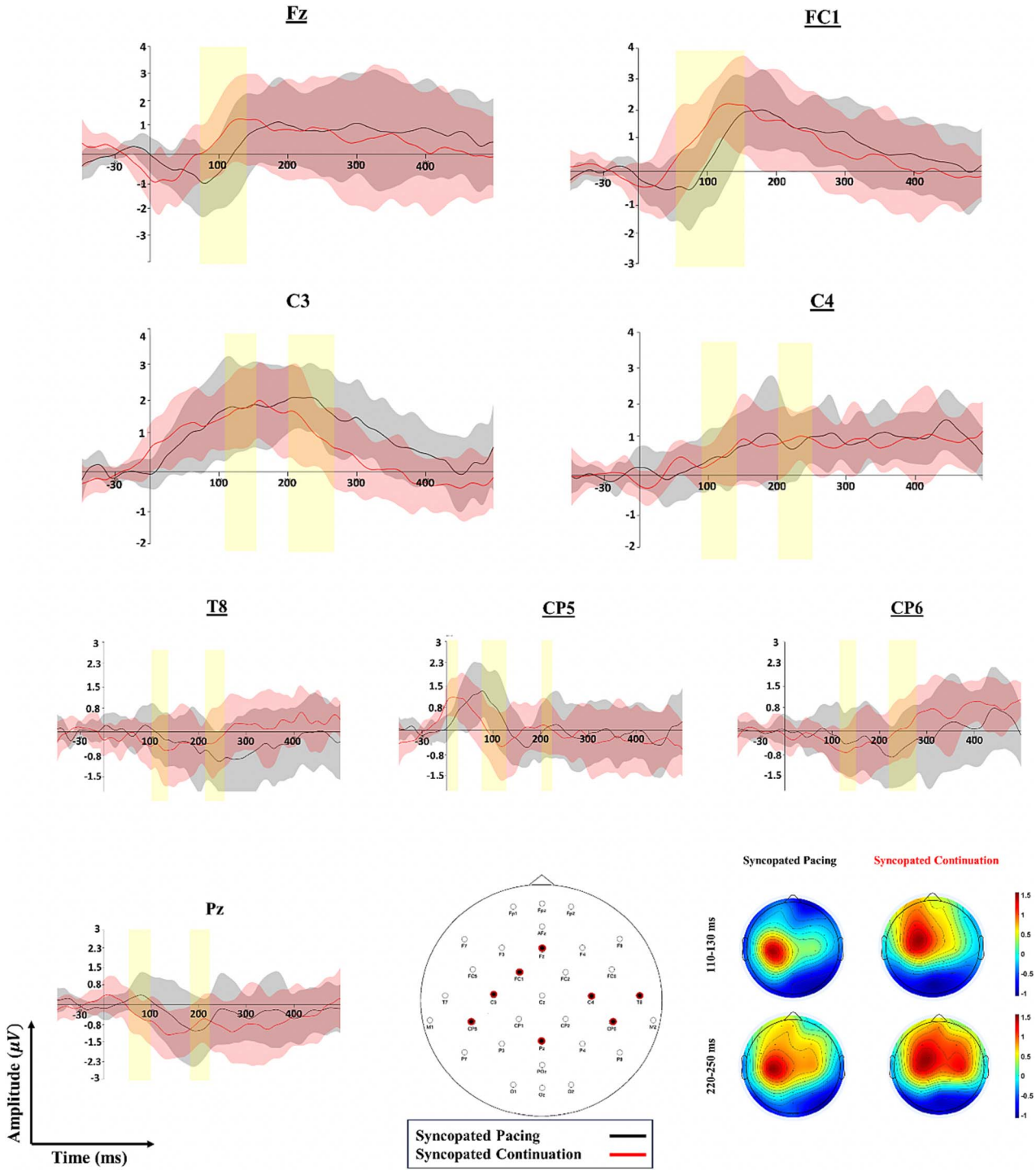

Fig. 9. Response-locked ERPs at the electrode sites contributing most to classification accuracy (syncopated pacing and syncopated continuation) in the deep learning model. The *x* axis indicates the time in ms after auditory tapping response-locked presentation. The curves indicate the averaged ERP values of pacing and continuation phases, respectively. The shading indicates the SE across the time. The *y* axis indicates the voltage in μV (note that the scaling of the *y* axis differs between the plots. The shading shows the time interval that was found to contribute strongly to classification performance in the deep learning network. The scalp maps in the bottom-right side indicate the amplitude of electrode sites in extracted motor components (time range: 110 to 130 ms and 220 to 250 ms). Please note that the *y* axis limits are scaled to the data amplitudes for each plot.

Discussion

Here, we investigated the neurophysiological activity corresponding to finger-tapping processes given systematic manipulation of tapping pattern (coordination mode) and phase in the continuation paradigm (pacing or continuation). Our findings go beyond conventional ERP component analyses to functionally relate EEG features to behavioral performance. We were able to achieve this at the time scale of single trials, demonstrating the neurophysiological processes corresponding to a single behavior.

Our results revealed temporal changes in tapping accuracy and precision across coordination modes, demonstrating that the more challenging timing condition to perform corresponds to the

Downloaded from https://academic.oup.com/cercor/article/34/10/bhae427/7848901 by UC - Merced user on 30 October 2024

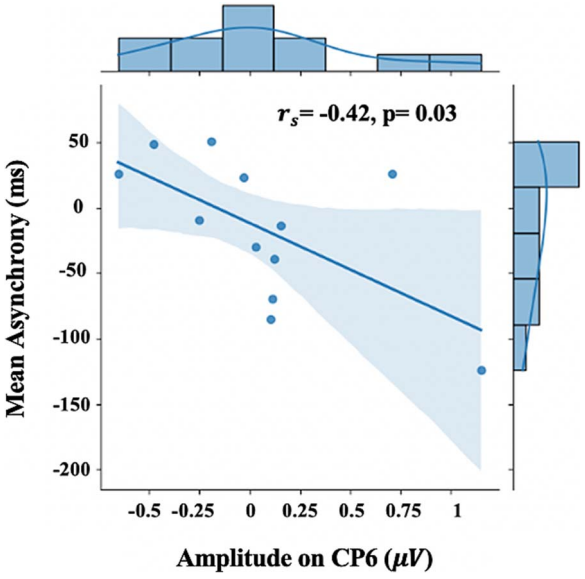

Fig. 10. Scatterplots showing individual indices of extracted auditory locked single-trial neural features corresponding to mean accuracy asynchrony in the synchronized pacing condition. The plot illustrates that behavioral accuracy improves with increasing negative amplitude of selective neural features in CP6.

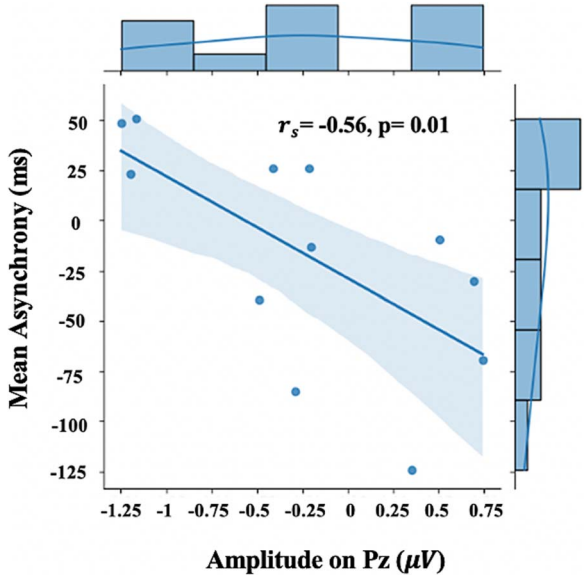

Fig. 12. Scatterplots showing individual indices of extracted response tapping–locked single-trial neural features corresponding to mean accuracy asynchrony in the syncopated continuation condition. The plot illustrates that behavioral accuracy improves with decreasing strength of amplitude of selective neural features in Pz.

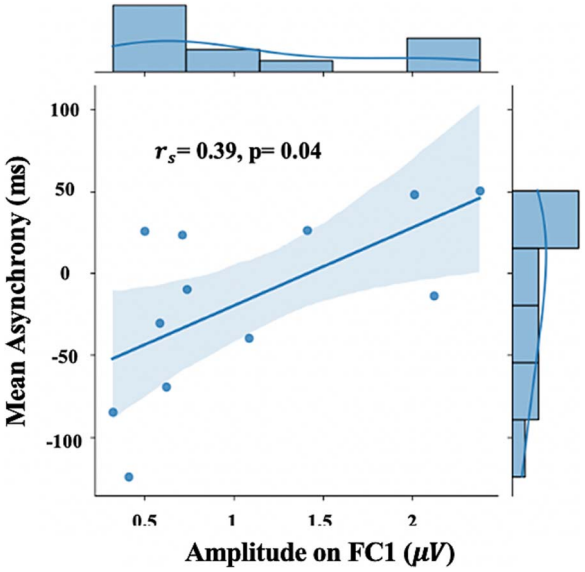

Fig. 11. Scatterplots showing individual indices of extracted response tapping–locked single-trial neural features corresponding to mean accuracy asynchrony in syncopated pacing condition. The plot illustrates that behavioral accuracy improves with increasing strength of amplitude of selective neural features in FC1.

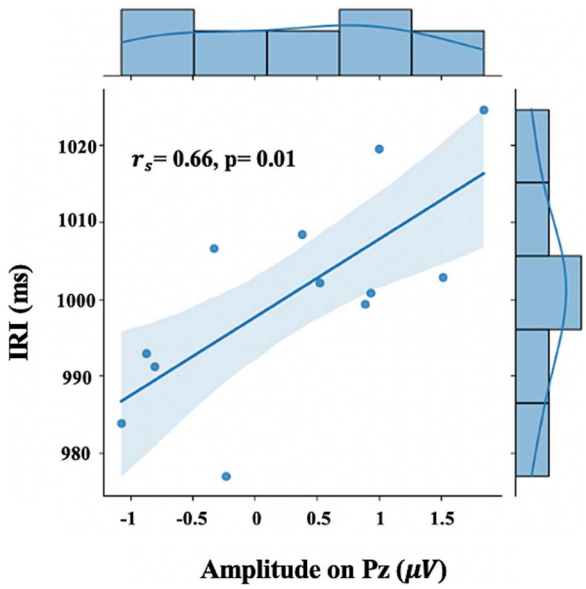

Fig. 13. Scatterplots showing individual indices of extracted auditory-locked single-trial neural features corresponding to IRI in syncopated pacing condition. The plot illustrates that behavioral accuracy improves with decreasing strength of amplitude of selective neural features in Pz.

lowest absolute tapping accuracy and precision. This could indicate that behavioral performance reflects the cognitive demand or effort required to perform the tapping task and that this demand is higher when the tapping pattern is more complex, for example, syncopation without a pacing stimulus. Alternatively, it could indicate that different asynchrony accuracy and IRI across time reflects the degree of mismatch or conflict between the produced rhythms with/without tones and that this mismatch is higher when the tapping pattern is more dissimilar or incongruent with the stimulus rhythm and particularly during the transition from pacing to continuation. These interpretations are consistent with previous studies that have shown increased neural activity and complexity in response to increased task difficulty or unpredictability in timing tasks (Chemin et al. 2014; Nozaradan et al. 2016; Comstock et al. 2018). Moreover, our findings suggest that different coordination modes may recruit different neural mechanisms for maintaining temporal accuracy and precision, as evidenced by the distinct patterns of EEG features extracted by our deep learning approach.

The central nervous system supports the dynamic behavior of the motor system for planning, controlling, and learning actions (Wolpert et al. 1995; Kawato 1999; Ashe et al. 2006), and listening to rhythmic sound sequences activates not only the auditory system but also the sensorimotor system (Fujioka et al. 2009).

Downloaded from https://academic.oup.com/cercor/article/34/10/bhae427/7848901 by UC - Merced user on 30 October 2024

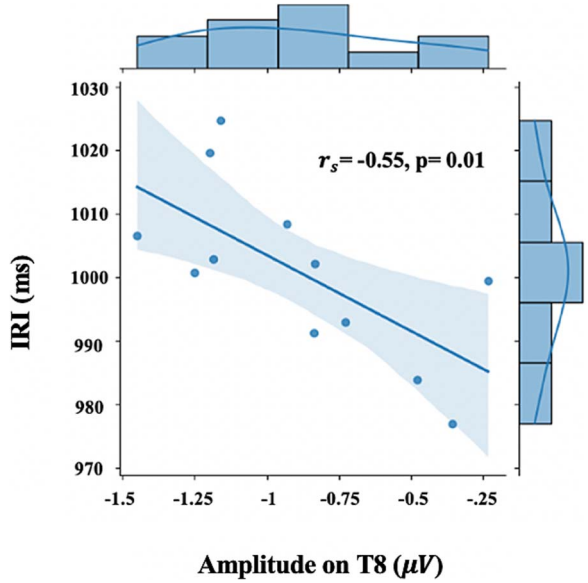

Fig. 14. Scatterplots showing individual indices of extracted response tapping–locked single-trial neural features corresponding to IRI in syncopated pacing condition. The plot illustrates that IRI behavioral accuracy may improve with decreasing strength of amplitude of selective neural features on T8.

Moreover, engagement of the inferior frontal lobule (supporting auditory–motor coupling) during synchronized pacing, and of the inferior parietal lobule during continuation, was observed by researchers using EEG frequency–based SSEPs (De Pretto et al. 2018). Pfurtscheller et al. (2003) found beta-band oscillation in the mid-central area, reflecting inhibition of neural subnetworks during synchronized continuation, and Ross et al. (2022) observed a significant role of mu rhythms in motor inhibition during beat perception.

The findings we report here demonstrate how neurophysiological activity corresponds to performance on our finger-tapping task, which in this case alternates in complexity from trial to trial. Electrophysiological activity is differentially modulated by specific movement parameters (Jäncke et al. 1998). Indeed, in the present study, each experimental condition activated a network compatible with the automatic, motor-related timing network, with additional contributions to motor coordination provided from frontal and central sites as required by different levels of timing complexity. This is consistent with our previous findings (Rahimpour et al. 2020), which demonstrated that increases in oxygenated hemoglobin (oxy-Hb) levels (indicating the amount of neurophysiological activity) corresponded to the degree of difficulty of the different timing behaviors.

The deep learning approach we implemented here revealed inherent differences between phases (pacing vs. continuation) by extracting meaningful contribution of ERP components and channels. This neural finding is consistent with the statistically significant contrast effects we observed in the behavioral results. The contrast of behavioral results reveals the superiority of mean accuracy asynchrony as compared to the IRI index in relation to the neural findings. In the stimulus-locked ERP waveforms, N1 and P2 peak latencies were significantly engaged in phase contrast in both synchronization and syncopation patterns. These two components are generally associated in the extant literature with sensory and perceptual processes, including sensory gating, selective attention, and stimulus identification (Fogarty et al. 2020). We also observed the contribution of response-locked single-trial features to sensorimotor electrode sites associated with motor responses, consistent with findings relating these electrode sites to sensory, motor-related, and attentional and working memory processes.

Findings from the current study provide insight into the neural basis of timing behavior by exploiting phases (pacing-continuation) of the continuation paradigm together with changes in coordination dynamics as introduced by the alternating design we implemented. The results indicate that neurophysiological correlates of cognitive processes in frontal, parietal, temporal, and central sites exhibit distinct markers that may be used to guide classification of trial phase in the continuation paradigm. The results provide promising evidence for neurally based predictions about the various neural processes in timed actions and provide a way of dealing with studying the cortical dynamics that might serve as the basis for motor equivalence. Thus, deep learning may expand our understanding of neural processes by guiding the generation of new hypotheses about timing behavior, including moving beyond conventional ERP components and functionally relating EEG features to behavioral timing performance.

In the post hoc power analysis using GPower software (Faul and Erdfelder 1992), our sample size of 12 was used, and a two-predictor variable equation (mode and phase) served as a baseline. Effect sizes were categorized as small (Cohen's $d = 0.14$), medium (Cohen's $d = 0.39$), and large (Cohen's $d = 0.59$). The study demonstrated sufficient statistical power (power = 0.8) for detecting moderate to large effect sizes but less than adequate power for detecting small effect sizes. The chosen significance level was $P < 0.05$ (α-level). Thus, while the study could reliably detect substantial effects, it may not be as sensitive to smaller effects.

While the EEGNet model successfully distinguished between pacing and continuation phases, it encountered challenges when attempting to differentiate between synchronization and syncopation coordination modes. These modes both involve auditory–motor integration and error correction processes but differ in their levels of complexity. One plausible explanation for the model's difficulties is the subtle neural activation differences between synchronization and syncopation, which may not have been captured effectively due to the limited sensitivity of the EEGNet model. This limitation could be attributed to the model being trained on a relatively small and noisy dataset, which lacked constraints or prior knowledge of specific neural patterns of interest. Additionally, the model may have overfitted to the more distinct pacing and continuation phases, which were more prominent in the data, while underperforming on the more transient and variable features associated with synchronization and syncopation.

To improve classification performance, we propose the following strategies : (i) employ alternative stimuli or tasks that can elicit more pronounced and consistent neural differences between synchronization and syncopation, such as using musical or speech stimuli or incorporating adaptive, interactive tasks and (ii) explore more advanced deep neural network architectures, such as recurrent neural networks or transfer learning, which may be better suited to capturing the subtle neural differences between the two modes. After removing auditory components from the EEG data, the classification accuracy between synchronization and syncopation further declined. This suggests that auditory cues play a critical role in driving the neural differentiation between these two coordination modes. Without the auditory input, the ability to classify these conditions became inconclusive, highlighting the importance of sensory input in distinguishing between motor timing strategies.

Downloaded from https://academic.oup.com/cercor/article/34/10/bhae427/7848901 by UC - Merced user on 30 October 2024

There are several limitations to be addressed in future research. First, the results of other classifications (between coordination modes) were inconclusive. Therefore, increasing sample size to improve the quality of the data that serves as the basis for the deep learning approach may improve overall classification performance. Second, although using deep learning further validates the interpretation of some of our findings, particularly that attentional, working memory, and sensorimotor components are in play to different degrees in the different phases of the continuation paradigm, there are still some uncertainties in predicting behavioral accuracy based on single-trial neurophysiological markers. Additional variables, encompassing motor planning, error monitoring, and feedback processing, might contribute to the observed disparities in EEG patterns among the conditions. The implications extend beyond the confines of attention and working memory as exclusive or principal cognitive functions implicated in sensorimotor synchronization. Further research will be needed to modify experimental tasks to directly target the association of these cognitive components and further refine these deep-learning models. We also suggest using connectivity analyses to identify the brain regions and networks associated with attention and working memory in sensorimotor synchronization. Third, more complex timing trials (Fitch and Rosenfeld 2007) and alternating designs may not accurately reflect the underlying neural activity in more extended timing scenarios (Rahimpour Jounghani et al. 2023). Dynamic alternation between complex actions may stymie our ability to reliably investigate neural activity associated within and across the various subsystems involved in pacing and continuation phases of action-based timing behavior.

Conclusion

This study explored the neurophysiological correlates of action-based timing behaviors using EEG and deep learning. Our findings demonstrate that neural activity, as measured by EEG, can accurately differentiate between pacing and continuation phases, particularly when auditory cues are present. The significant classification accuracy observed during the pacing phase underscores the critical role of auditory stimuli in guiding motor timing behaviors. However, when auditory components were removed from the data, the classification of motor activation across phases became inconclusive, suggesting that the auditory input may be a key driver of the observed differentiation effects.

The results emphasize the challenges of isolating motor-related neural responses in the absence of external auditory cues. The superior performance of mean accuracy asynchrony, compared to the IRI index, highlights the relevance of this measure in reflecting the neural findings associated with timing behaviors. Future research should focus on further disentangling the contributions of auditory and motor components to timing behaviors and explore how different sensory modalities influence motor coordination in complex timing tasks.

Author contributions

Ali Rahimpour Jounghani (Conceptualization, Data curation, Formal analysis, Methodology, Resources, Software, Visualization, Writing—original draft, Writing—review & editing), Kristina Backer (Data curation, Formal analysis, Methodology, Resources, Software, Writing—review & editing), Amirali Vahid (Data curation, Formal analysis, Methodology, Software, Writing—review & editing), Daniel Comstock (Data curation, Formal analysis, Software, Writing—review & editing), Jafar Zamani (Formal analysis), SM Hadi Hosseini (Formal analysis, Methodology, Software, Writing—review & editing), Ramesh Balasubramaniam (Conceptualization, Funding acquisition, Resources, Writing—review & editing), and Heather Bortfeld (Conceptualization, Funding acquisition, Investigation, Project administration, Resources, Supervision, Writing—review & editing).

Funding

The work was partially supported by NIH/NIDCD R01DC010075 & NIH/NHLBI 1R01HL167012 to H.B. and by NSFBCS 1460633, NSF DGE 1633722 to R.B. A.R.J.'s effort was partly supported by the NIH T32 Postdoctoral Fellowship in the Center for Interdisciplinary Brain Sciences Research.

Conflict of interest statement: None declared.

References

Ashe J, Lungu OV, Basford AT, Lu X. Cortical control of motor sequences. *Curr Opin Neurobiol*. 2006:16:213–221. https://doi.org/10.1016/j.conb.2006.03.008.

Bavassi L, Kamienkowski JE, Sigman M, Laje R. Sensorimotor synchronization: neurophysiological markers of the asynchrony in a finger-tapping task. *Psychol Res*. 2017:81:143–156. https://doi.org/10.1007/s00426-015-0721-6.

Bell AJ, Sejnowski TJ. An information-maximization approach to blind separation and blind deconvolution. *Neural Comput*. 1995:7:1129–1159. https://doi.org/10.1162/neco.1995.7.6.1129.

Boonstra TW, Daffertshofer A, Peper CE, Beek PJ. Amplitude and phase dynamics associated with acoustically paced finger tapping. *Brain Res*. 2006:1109:60–69. https://doi.org/10.1016/j.brainres.2006.06.039.

Chemin B, Mouraux A, Nozaradan S. Body movement selectively shapes the neural representation of musical rhythms. *Psychol Sci*. 2014:25:2147–2159. https://doi.org/10.1177/0956797614551161.

Chen JL, Penhune VB, Zatorre RJ. Listening to musical rhythms recruits motor regions of the brain. *Cereb Cortex*. 2008:18:2844–2854. https://doi.org/10.1093/cercor/bhn042.

Clark CR, Moores KA, Lewis A, Weber DL, Fitzgibbon S, Greenblatt R, Taylor J. Cortical network dynamics during verbal working memory function. *Int J Psychophysiol*. 2001:42:161–176. https://doi.org/10.1016/S0167-8760(01)00164-7.

Collective BSM, Shaw D. Makey Makey: Improvising tangible and nature-based user interfaces. In: Fishkin KP, Grossman T, Hudson SE, Tan DS, editors. *Proceedings of the Sixth International Conference on Tangible, Embedded and Embodied Interaction*. New York, NY: Association for Computing Machinery; 2012. p. 367–370. https://doi.org/10.1145/2148131.2148219.

Comstock DC, Balasubramaniam R. Neural responses to perturbations in visual and auditory metronomes during sensorimotor synchronization. *Neuropsychologia*. 2018:117:55–66. https://doi.org/10.1016/j.neuropsychologia.2018.05.013.

Comstock DC, Hove MJ, Balasubramaniam R. Sensorimotor synchronization with auditory and visual modalities: Behavioral and neural differences. *Front Comput Neurosci*. 2018:12:53. https://doi.org/10.3389/fncom.2018.00053.

Davranche K, Nazarian B, Vidal F, Coull J. Orienting attention in time activates left intraparietal sulcus for both perceptual and motor task goals. *J Cogn Neurosci*. 2011:23:3318–3330. https://doi.org/10.1162/jocn_a_00030.

Downloaded from https://academic.oup.com/cercor/article/34/10/bhae427/7848901 by UC - Merced user on 30 October 2024

De Pretto M, Deiber M-P, James CE. Steady-state evoked potentials distinguish brain mechanisms of self-paced versus synchronization finger tapping. *Hum Mov Sci*. 2018:61:151–166. https://doi.org/10.1016/j.humov.2018.07.007.

Delorme A, Makeig S. EEGLAB: an open source toolbox for analysis of single-trial EEG dynamics including independent component analysis. *J Neurosci Methods*. 2004:134:9–21. https://doi.org/10.1016/j.jneumeth.2003.10.009.

Drake C, Jones MR, Baruch C. The development of rhythmic attending in auditory sequences: attunement, referent period, focal attending. *Cognition*. 2000:77:251–288. https://doi.org/10.1016/S0010-0277(00)00106-2.

Ebrahimzadeh E, Shams M, Jounghani AR, Fayaz F, Mirbagheri M, Hakimi N, Soltanian-Zadeh H. Epilepsy presurgical evaluation of patients with complex source localization by a novel component-based EEG-fMRI approach. *Iran J Radiol*. 2019:16(1):e99134. https://doi.org/10.5812/iranjradiol.99134.

Ebrahimzadeh E, Shams M, Jounghani AR, Fayaz F, Mirbagheri M, Hakimi N, Soltanian-Zadeh H. Localizing confined epileptic foci in patients with an unclear focus or presumed multifocality using a component-based EEG-fMRI method. *Cogn Neurodyn*. 2020:14(1):1–16.

Ebrahimzadeh E, Shams M, Seraji M, Sadjadi SM, Rajabion L, Soltanian-Zadeh H. Localizing epileptic foci using simultaneous EEG-fMRI recording: template component cross-correlation. *Front Neurol*. 2021:12:695997. https://doi.org/10.3389/fneur.2021.695997.

Eimer M. The lateralized readiness potential as an on-line measure of central response activation processes. *Behav Res Methods Instrum Comput*. 1998:30:146–156. https://doi.org/10.3758/BF03209424.

Erdfelder E, Faul F, Buchner A. GPOWER: A general power analysis program. *Behavior Research Methods, Instruments, & Computers*. 1996:28:1–11. New York, NY: Springer. https://doi.org/10.3758/BF03203630.

Fitch WT, Rosenfeld AJ. Perception and production of syncopated rhythms. *Music Percept*. 2007:25:43–58. https://doi.org/10.1525/mp.2007.25.1.43.

Fogarty JS, Barry RJ, Steiner GZ. Auditory stimulus-and response-locked ERP components and behavior. *Psychophysiology*. 2020:57:e13538. https://doi.org/10.1111/psyp.13538.

Fujioka T, Trainor LJ, Large EW, Ross B. Beta and gamma rhythms in human auditory cortex during musical beat processing. *Ann N Y Acad Sci*. 2009:1169:89–92. https://doi.org/10.1111/j.1749-6632.2009.04779.x.

Grahn JA, Brett M. Rhythm and beat perception in motor areas of the brain. *J Cogn Neurosci*. 2007:19:893–906. https://doi.org/10.1162/jocn.2007.19.5.893.

Harrington DL, Haaland KY, Knight RT. Cortical networks underlying mechanisms of time perception. *J Neurosci*. 1998:18:1085–1095. https://doi.org/10.1523/JNEUROSCI.18-03-01085.1998.

Hove MJ, Fairhurst MT, Kotz SA, Keller PE. Synchronizing with auditory and visual rhythms: an fMRI assessment of modality differences and modality appropriateness. *NeuroImage*. 2013:67:313–321. https://doi.org/10.1016/j.neuroimage.2012.11.032.

Ivry RB, Keele SW. Timing functions of the cerebellum. *J Cogn Neurosci*. 1989:1:136–152. https://doi.org/10.1162/jocn.1989.1.2.136.

Ivry RB, Spencer RMC. The neural representation of time. *Curr Opin Neurobiol*. 2004:14:225–232. https://doi.org/10.1016/j.conb.2004.03.013.

Jäncke L, Specht K, Mirzazade S, Loose R, Himmelbach M, Lutz K, Shah NJ. A parametric analysis of therate effect'in the sensorimotor cortex: a functional magnetic resonance imaging analysis in human subjects. *Neurosci Lett*. 1998:252:37–40. https://doi.org/10.1016/S0304-3940(98)00540-0.

Jantzen KJ, Kelso JAS. Neural coordination dynamics of human sensorimotor behavior: A review. In: Jirsa V, McIntosh AR, editors. *Handbook of brain connectivity*. Berlin, Heidelberg: Springer; 2007. p. 421–461. https://doi.org/10.1007/978-3-540-71512-2_15.

Jantzen KJ, Steinberg FL, Kelso JAS. Brain networks underlying human timing behavior are influenced by prior context. *Proc Natl Acad Sci*. 2004:101:6815–6820. https://doi.org/10.1073/pnas.0401300101.

Kappenman ES, Luck SJ. The effects of electrode impedance on data quality and statistical significance in ERP recordings. *Psychophysiology*. 2010:47:888–904. https://doi.org/10.1111/j.1469-8986.2010.01009.x.

Kawato M. Internal models for motor control and trajectory planning. *Curr Opin Neurobiol*. 1999:9:718–727. https://doi.org/10.1016/S0959-4388(99)00028-8.

Kelso JS, Fuchs A, Lancaster R, Holroyd T, Cheyne D, Weinberg H. Dynamic cortical activity in the human brain reveals motor equivalence. *Nature*. 1998:392:814–818. https://doi.org/10.1038/33922.

Kingma DP, Ba J. Adam: a method for stochastic optimization. *Proceedings of the 3rd International Conference on Learning Representations (ICLR)*; 2015. p. 1–15. Available from: arXiv preprint arXiv:1412.6980.

Lashley KS. Basic neural mechanisms in behavior. *Psychol Rev*. 1930:37:1–24. https://doi.org/10.1037/h0074134.

Lewis PA, Wing AM, Pope PA, Praamstra P, Miall RC. Brain activity correlates differentially with increasing temporal complexity of rhythms during initialisation, synchronisation, and continuation phases of paced finger tapping. *Neuropsychologia*. 2004:42:1301–1312. https://doi.org/10.1016/j.neuropsychologia.2004.03.001.

Lopez-Calderon J, Luck SJ. ERPLAB: an open-source toolbox for the analysis of event-related potentials. *Front Hum Neurosci*. 2014:8:213. https://doi.org/10.3389/fnhum.2014.00213.

Makeig S, Debener S, Onton J, Delorme A. Mining event-related brain dynamics. *Trends Cogn Sci*. 2004:8:204–210. https://doi.org/10.1016/j.tics.2004.03.008.

Mathias B, Zamm A, Gianferrara PG, Ross B, Palmer C. Rhythm complexity modulates behavioral and neural dynamics during auditory–motor synchronization. *J Cogn Neurosci*. 2020:32:1864–1880. https://doi.org/10.1162/jocn_a_01601.

Mayville JM, Bressler SL, Fuchs A, Kelso JAS. Spatiotemporal reorganization of electrical activity in the human brain associated with a timing transition. *Exp Brain Res*. 1999:127:371–381. https://doi.org/10.1007/s002210050805.

Mayville JM, Jantzen KJ, Fuchs A, Steinberg FL, Kelso JAS. Cortical and subcortical networks underlying syncopated and synchronized coordination revealed using fMRI. *Hum Brain Mapp*. 2002:17:214–229. https://doi.org/10.1002/hbm.10065.

Näätänen R, Picton T. The N1 wave of the human electric and magnetic response to sound: a review and an analysis of the component structure. *Psychophysiology*. 1987:24:375–425. https://doi.org/10.1111/j.1469-8986.1987.tb00311.x.

Nachev P, Kennard C, Husain M. Functional role of the supplementary and pre-supplementary motor areas. *Nat Rev Neurosci*. 2008:9:856–869. https://doi.org/10.1038/nrn2478.

Nave KM, Hannon EE, Snyder JS. Steady state-evoked potentials of subjective beat perception in musical rhythms. *Psychophysiology*. 2022:59:e13963. https://doi.org/10.1111/psyp.13963.

Nobre AC. Orienting attention to instants in time. *Neuropsychologia*. 2001:39:1317–1328. https://doi.org/10.1016/S0028-3932(01)00120-8.

Downloaded from https://academic.oup.com/cercor/article/34/10/bhae427/7848901 by UC - Merced user on 30 October 2024

Nozaradan S, Peretz I, Keller PE. Individual differences in rhythmic cortical entrainment correlate with predictive behavior in sensorimotor synchronization. *Sci Rep*. 2016:6:20612. https://doi.org/10.1038/srep20612.

Pabst A, Balasubramaniam R. Trajectory formation during sensorimotor synchronization and syncopation to auditory and visual metronomes. *Exp Brain Res*. 2018:236:2847–2856. https://doi.org/10.1007/s00221-018-5343-y.

Paek AY, Agashe H, Contreras-Vidal JL. Decoding repetitive finger movements with brain activity acquired via non-invasive electroencephalography. *Front Neuroeng*. 2014:7:3. https://doi.org/10.3389/fneng.2014.00003.

Peper CE, Beek PJ, van Wieringen PCW. Multifrequency coordination in bimanual tapping: asymmetrical coupling and signs of supercriticality. *J Exp Psychol Hum Percept Perform*. 1995:21:1117.

Pfurtscheller G, Woertz M, Supp G, da Silva FHL. Early onset of post-movement beta electroencephalogram synchronization in the supplementary motor area during self-paced finger movement in man. *Neurosci Lett*. 2003:339:111–114. https://doi.org/10.1016/S0304-3940(02)01479-9.

Rahimpour Jounghani A, Lanka P, Pollonini L, Proksch S, Balasubramaniam R, Bortfeld H. Multiple levels of contextual influence on action-based timing behavior and cortical activation. *Sci Rep*. 2023:13:7154. https://doi.org/10.1038/s41598-023-33780-1.

Rahimpour A, Pollonini L, Comstock D, Balasubramaniam R, Bortfeld H. Tracking differential activation of primary and supplementary motor cortex across timing tasks: an fNIRS validation study. *J Neurosci Methods*. 2020:341:108790. https://doi.org/10.1016/j.jneumeth.2020.108790.

Refaeilzadeh P, Tang L, Liu H. Cross-validation. *Encyclopedia of database systems*. 2009:5:532–538. https://doi.org/10.1007/978-0-387-39940-9_565.

Repp BH. Sensorimotor synchronization: a review of the tapping literature. *Psychon Bull Rev*. 2005:12:969–992. https://doi.org/10.3758/BF03206433.

Rizzolatti G, Luppino G. The cortical motor system. *Neuron*. 2001:31:889–901. https://doi.org/10.1016/S0896-6273(01)00423-8.

Ross JM, Comstock DC, Iversen JR, Makeig S, Balasubramaniam R. Cortical mu rhythms during action and passive music listening. *J Neurophysiol*. 2022:127:213–224. https://doi.org/10.1152/jn.00346.2021.

Sadjadi SM, Ebrahimzadeh E, Shams M, Seraji M, Soltanian-Zadeh H. Localization of epileptic foci based on simultaneous EEG–fMRI data. *Front Neurol*. 2021:12:645594. https://doi.org/10.3389/fneur.2021.645594.

Seabold S, Perktold J. Statsmodels: econometric and statistical modeling with Python. *Proceedings of the 9th Python in Science Conference (SciPy)*; 2010. p. 92–96.

Sergent J. Mapping the musician brain. *Hum Brain Mapp*. 1993:1:20–38. https://doi.org/10.1002/hbm.460010104.

Serrien DJ. The neural dynamics of timed motor tasks: evidence from a synchronization–continuation paradigm. *Eur J Neurosci*. 2008:27:1553–1560. https://doi.org/10.1111/j.1460-9568.2008.06110.x.

Simonyan K, Vedaldi A, Zisserman A. Deep inside convolutional networks: visualising image classification models and saliency maps. *Proceedings of the 2nd International Conference on Learning Representations (ICLR)*; 2014. p. 1–8. Available from: arXiv preprint arXiv:1312.6034.

Smit DJA, Linkenkaer-Hansen K, de Geus EJC. Long-range temporal correlations in resting-state alpha oscillations predict human timing-error dynamics. *J Neurosci*. 2013:33:11212–11220. https://doi.org/10.1523/JNEUROSCI.2816-12.2013.

Smith EE, Jonides J. Neuroimaging analyses of human working memory. *Proc Natl Acad Sci*. 1998:95:12061–12068. https://doi.org/10.1073/pnas.95.20.12061.

Spencer NJ, Bywater RAR, Holman ME, Taylor GS. Inhibitory neurotransmission in the circular muscle layer of mouse colon. *J Auton Nerv Syst*. 1998:70:10–14. https://doi.org/10.1016/S0165-1838(98)00045-9.

Vahid A, Bluschke A, Roessner V, Stober S, Beste C. Deep learning based on event-related EEG differentiates children with ADHD from healthy controls. *J Clin Med*. 2019:8:1055. https://doi.org/10.3390/jcm8071055.

Vahid A, Mückschel M, Stober S, Stock AK, Beste C. Applying deep learning to single-trial EEG data provides evidence for complementary theories on action control. *Commun Biol*. 2020:3:112. https://doi.org/10.1038/s42003-020-0846-z.

Van Diepen RM, Mazaheri A. The caveats of observing inter-trial phase-coherence in cognitive neuroscience. *Sci Rep*. 2018:8:2990. https://doi.org/10.1038/s41598-018-20423-z.

Wallenstein GV, Kelso JAS, Bressler SL. Phase transitions in spatiotemporal patterns of brain activity and behavior. *Physica D*. 1995:84:626–634. https://doi.org/10.1016/0167-2789(95)00056-A.

Wing AM, Kristofferson AB. Response delays and the timing of discrete motor responses. *Percept Psychophys*. 1973:14:5–12. https://doi.org/10.3758/BF03198607.

Witt ST, Laird AR, Meyerand ME. Functional neuroimaging correlates of finger-tapping task variations: an ALE meta-analysis. *NeuroImage*. 2008:42:343–356. https://doi.org/10.1016/j.neuroimage.2008.04.025.

Wolpert DM, Ghahramani Z. Computational principles of movement neuroscience. *Nat Neurosci*. 2000:3:1212–1217. https://doi.org/10.1038/81497.

Wolpert DM, Ghahramani Z, Jordan MI. An internal model for sensorimotor integration. *Science*. 1995:269:1880–1882. https://doi.org/10.1126/science.7569931.

Downloaded from https://academic.oup.com/cercor/article/34/10/bhae427/7848901 by UC - Merced user on 30 October 2024